

Article

Interdisciplinary Approach and Geodynamic Implications of the Goutitir Geothermal System (Eastern Meseta, Morocco)

El Mehdi Jeddi ¹, Ahmed Ntarmouchant ¹, Maria do Rosário Carvalho ^{2,3,*}, Telmo M. Bento dos Santos ^{2,3}, Eduardo Anselmo Ferreira da Silva ⁴, Mustapha Elabouyi ⁵, Youssef Driouch ¹, Brahim Mali ¹, Nahla Ntarmouchant ⁶, My Hachem Smaili ¹, Beatriz Cotrim ² and Mohamed Dahire ¹

¹ GERA—Laboratory of Geosciences, Environment and Associated Resources, Faculty of Sciences, University Sidi Mohammed Ben Abdellah, Dhar El Mehraz, Fez 30050, Morocco

² Instituto Dom Luiz (IDL), Faculdade de Ciências, Universidade de Lisboa, Campo Grande, 1749-016 Lisboa, Portugal

³ DG-FCUL—Departamento de Geologia, Faculdade de Ciências, Universidade de Lisboa, Campo Grande, Edifício C6, 1749-016 Lisboa, Portugal

⁴ GeoBioTec Research Unit, Department of Geosciences, University of Aveiro, Campus de Santiago, 3810-193 Aveiro, Portugal

⁵ Faculty of Sciences, Moulay Ismail University, Meknes 50000, Morocco

⁶ DLGR Laboratory, URAC 43, Faculty of Sciences Semlalia, Cadi Ayyad University, Marrakech 40000, Morocco

* Correspondence: mdrcarvalho@fc.ul.pt

Abstract: Morocco has an important geothermal potential materialized by its several thermal springs which constitute an essential surface geothermal indicator. These springs are dispersed throughout the country and present in every major structural domain. However, a significant amount is concentrated in the northern and northeastern areas. Associated with the great hydrothermal system of eastern Morocco, the thermal spring of Goutitir emerges in the Meso-Cenozoic sedimentary formations located east of the Guercif Basin, composed of a mixture of clays, carbonates, and marls, covered in unconformity by Quaternary tabular molasses. The upflow of the thermal water is dependent of Alpine faults systems with N30 and N100 directions, which are probable reactivated Hercynian structures that facilitate its circulation to the surface. The Goutitir spring has been studied by an interdisciplinary approach to identify the origin of the thermal water, the rock–water interactions, and the reservoir temperatures, contributing to the establishment of the conceptual model of the associated hydrothermal system. This thermal water is of chloride-sodium type with a hyperthermal character (43–47 °C). The isotopic composition ($\delta^{18}\text{O} = -8.7$ to -8.35‰ ; $\delta^2\text{H} = -58.6$ to -54.3‰) indicates a meteoric origin and a recharging zone located at around 2000 m of altitude. The chemical composition allows to classify the water as chloride-sodium hydrochemical facies, stabilized at ~ 100 °C in crystalline basement rocks, which, according to seismic data, are located at ~ 3 km depth. The concentrations, patterns, and correlations of trace elements point out water–rock interaction processes between the deep water and basic magmatic rocks. The integration of the chemical and isotopic data and the surface geological context shows that the Goutitir water flows within a hydrothermal zone were basic to ultrabasic lamprophyres rich in gabbroic xenoliths outcrop, witnessing the existence, at depth, of basic plutons. Moreover, near the source, these veins are strongly altered and hydrothermalized, showing late recrystallization of centimetric-sized biotites. The chloride-sodium composition of this water may also be a testimony to the presence and reaction with the overlying Triassic saline and gypsiferous and Meso-Cenozoic mainly carbonated formations.

Keywords: Eastern Meseta; Goutitir thermal spring; geothermal system; chemical composition; stable isotopes

1. Introduction

In recent years, the concern for the use of green energies has led to an increase in geothermal resources exploration, which has been a new area of research in countries that



Citation: Jeddi, E.M.; Ntarmouchant, A.; Carvalho, M.d.R.; Bento dos Santos, T.M.; Ferreira da Silva, E.A.; Elabouyi, M.; Driouch, Y.; Mali, B.; Ntarmouchant, N.; Smaili, M.H.; et al. Interdisciplinary Approach and Geodynamic Implications of the Goutitir Geothermal System (Eastern Meseta, Morocco). *Water* **2023**, *15*, 1109. <https://doi.org/10.3390/w15061109>

Academic Editor: Paolo Madonia

Received: 21 January 2023

Revised: 3 March 2023

Accepted: 8 March 2023

Published: 14 March 2023



Copyright: © 2023 by the authors. Licensee MDPI, Basel, Switzerland. This article is an open access article distributed under the terms and conditions of the Creative Commons Attribution (CC BY) license (<https://creativecommons.org/licenses/by/4.0/>).

have a high potential for its exploitation [1–4]. Thermal springs are important surface clues for geothermal exploration. Morocco is a country with small relevance regarding fossil energy, but it has more than one hundred thermal springs, two-thirds of which are concentrated in the northern part of the country, in particular in the Rif Belt and the Meseta-Atlas domain. There is a strong connection between these thermal springs and active deep tectonic structures, which constitute preferential circulation routes for thermal waters (e.g., [5–8]). The study of these thermal springs is of great importance to understanding their origin and characteristics, contributing to the definition of the conceptual model of the geothermal reservoir. Their economic relevance is also not negligible, making these renewable, permanent, and easily exploitable energy sources, a good investment for a sustainable future.

In Morocco, the Eastern Meseta is considered a major hydrothermal province due to a large number of geothermal surface manifestations, namely Plio-Quaternary volcanism, neotectonic activity, and a high surface geothermal gradient ($>35\text{ }^{\circ}\text{C.km}^{-1}$; [9]), which favors the appearance of many thermal springs, especially those that emerge from Jurassic limestones such as Gufait, Fezouane, Kiss, and Ben Kachour and those whose discharge is located at the level of Neogene formations such as Goutitir (Figure 1A). The Neogene basins of the Eastern Meseta are the Guercif basin located in the northwest and the Taourirt-Oujda basin located in its northeast part. In the Neogene Guercif basin, there is only one thermal spring; it is the spring of Goutitir, the subject of this work. As the other thermal springs of the Eastern Meseta have an incomplete trace analysis, the Goutitir spring will be compared with thermal springs in the different Moroccan structural domains, notably the Oulmes (emerging at the Paleozoic basement of the western meseta) and Ain Alah (rising at the Southern Rifain Sillon) (Figure 1A).

Thermal waters carry important chemical information collected during their circulation through deep reservoirs and their transfer to the surface [10,11]. During this sometimes long-term circulation, processes of chemical diffusion between these waters and the circulated rocks take place. These water–rock interactions, occurring at depth, are controlled by physico-chemical balances which induce the enrichment of the thermal water in certain chemical elements, depending on the intersected lithologies at depth [8,12,13]. The geochemical study of these waters constitutes an important tool that allows the dissection of this information in order to determine their origin, the identification of the deep circulation paths, the estimation of the depth of the intersected lithospheric reservoirs, and the water/rock interactions that happened during the evolution of the thermo-mineral waters. This also includes the acquisition of data that allow the determination of the altitude and the location of the refill zones.

This study is focused on the geochemical and isotopic characteristics of these thermal waters and their relation with the geological and tectonic framework of the region, contributing to the conceptual model of the deep thermal reservoir. In addition to the geochemical data produced in this work, previous data will also be used, namely data from works carried out since 2000 ([5,14–16], this work, 2019). This will allow constraining the long-term geochemical variation of these thermal waters over a period of 19 years (collected from 2000 to 2019).

With this new vision, this study brings new results which could lead to the understanding of the origin and evolution of these thermal waters, as well as their hydrodynamic circulation pattern. It will focus mainly on the water–rock interaction using various indicators, such as the geochemistry and the isotopic composition of the water. The geological and tectonic contexts will allow the understanding of the different geodynamic mechanisms that favored the circulation of these thermal waters in depth and their upflow to the surface, as well as provide important clues as to the geological nature of the deep lithospheric reservoirs accessed by these thermal waters.

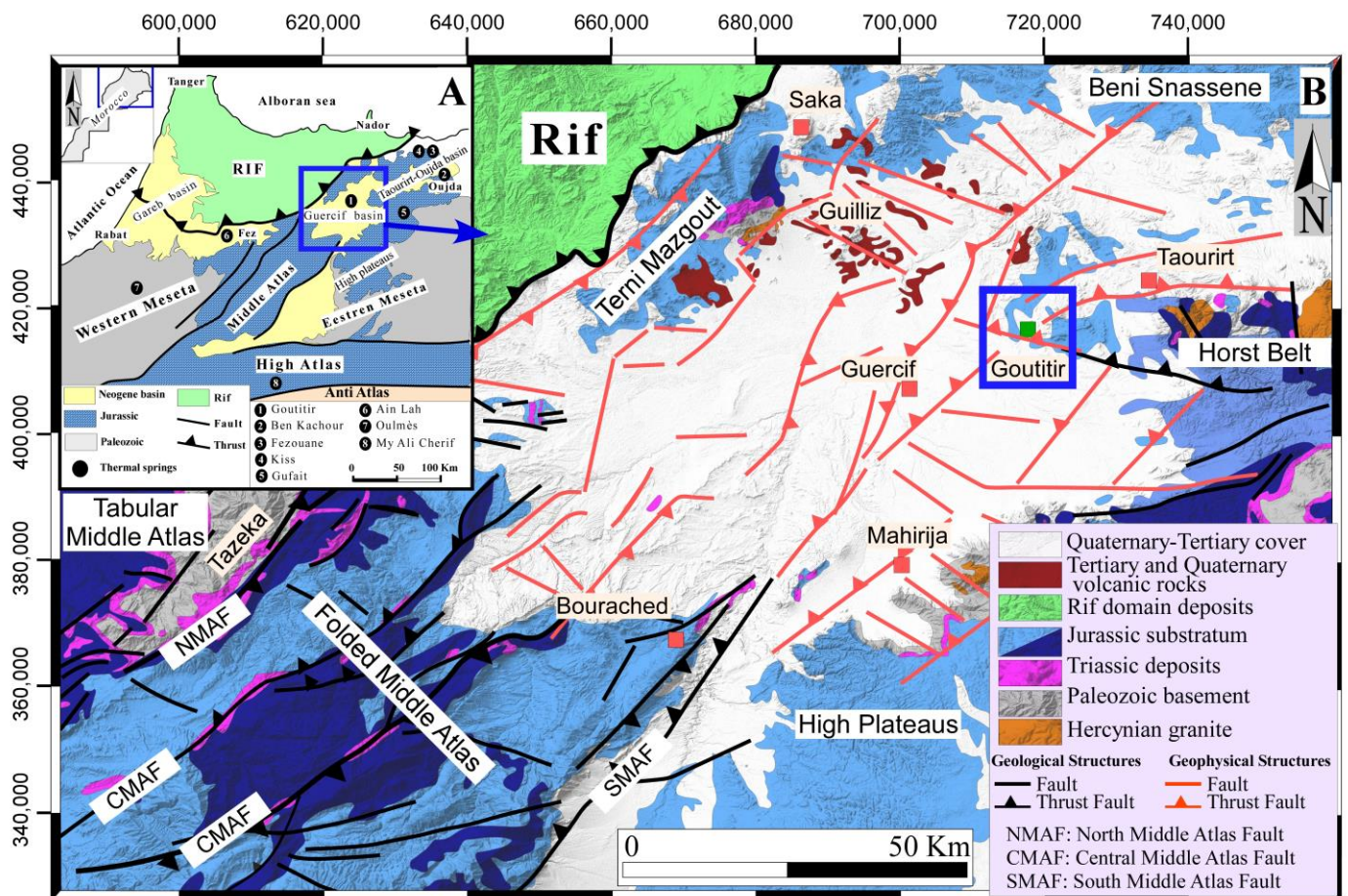


Figure 1. (A) Schematic geological map of northern Morocco showing the structural domains and location of a few thermal springs. (B) Geological map of the Guercif Basin and the neighboring region, modified from the geological map of Morocco at 1:1,000,000 scale [17].

2. Regional Geologic Setting

The Guercif basin corresponds to a vast depression of about 6000 km², oriented NE-SW, and considered an eastern extension of the South Rif Thrust (Figure 1B). It is bounded, respectively, to the northwest and the north by the Prerifan nappes and the Jurassic reliefs of Terni Mezgout, to the south by the Folded Middle Atlas, and to the east by the high plateaus of the Atlas belt (Figure 1B). This basin, of Neogene age, is characterized by successive magmatic manifestations from the collapse of the Atlas Belt, namely Eocene alkaline lamprophyres in the region of Taourirt and Plio-Quaternary calc-alkaline and alkaline lavas in the region of Guelliz. This basin is also characterized by a high thermal gradient, manifested by the occurrence of thermal springs in the south at Bourached, in the north at Goutitir (object of this work), and in the northwest, near Saka. This carbonate basin is delimited by NE-SW and ESE-WNW faults that are also responsible for the outcropping of nearby Paleozoic formations, as well as of Triassic and Jurassic sediments (Figure 1B). The Paleozoic basement is essentially composed of sandstone-pelitic metasedimentary formations deformed during the Hercynian Orogeny and intruded by Hercynian to late-Hercynian granitoids [18]. In the angular unconformity of the Paleozoic formations, the Triassic series (400–500 m) are composed of red detrital and clayey-evaporitic saline deposits, intercalated with basaltic flows [19–21]. Triassic formations can also appear in the form of isolated mounds linked to evaporitic diapiric upwellings at the level of major accidents traversing the Middle Atlas [22–24]. These reliefs are very common in this basin, particularly in Goutitir, Jbel Tirremi, and Koudiat Titeft (Figure 1). The Jurassic distension reactivated several Hercynian faults and led to the collapse of the region, with the formation

of sedimentary basins in NE–SW- and E–W-oriented grabens and half-grabens [21,25,26], where detrital formations materialized by alternating Jurassic sandstone and silty clays were deposited [27–29]. Core drillings in the region confirm that the Neogene formations are ~1500 m thick and deposited over the Jurassic rocks. This Neogene series begins with continental conglomerates and sandstones, followed by Tortonian gypsiferous blue marls [30,31]. The Quaternary cover is composed of conglomerates, tuffs, clays, and alluvial and fluvial silty terraces, as well as cliff fragments [32].

3. Methodology

Geological mapping and structural analysis were based on a preliminary analysis of Google Earth satellite images and followed up by a field campaign for structural analysis that was carried out in the studied area. This methodology allowed the understanding of the distribution of the different lithologies, as well as the tectonic structures affecting this region. Sorting and computer processing of structural measurements was carried out using the SG2PS software [33].

To better understand the variations of the physico-chemical composition of the thermal water of Goutitir, sampling, and chemical and isotopic analysis were performed. We also added to this study chemical analyses of previous works, spread over a period of 19 years ([5,14–16]; this work, 2019). Comparisons with data from our predecessors over the 19-year period show little or no change in the chemical compositions of these waters. Therefore, we considered that multiple samplings within the same source were not necessary.

The Goutitir water was sampled in July 2019. The samples were taken in polyethylene bottles, previously rinsed with the spring water. Measurements of some physico-chemical parameters (Temperature, Electrical Conductivity, Total Dissolved Solids, and pH) were carried out in situ, using a HANNA HI98194 Multi-parameter device.

Chemical analyses were performed at Actlabs Laboratories (Canada). Cations and metals were analyzed by ICP-MS, and ICP-OES (overrange elements), where anions were analyzed by potentiometry and ion chromatography. The isotopic composition of the water was determined at a C²TN/IST laboratory. The $\delta^2\text{H}$ and $\delta^{18}\text{O}$ measurements (vs. V-SMOW) were performed by laser spectroscopic analysis (LGR-24d from Los Gatos Research), with the accuracy of $\pm 1\%$ for $\delta^2\text{H}$ and $\pm 0.1\%$ for $\delta^{18}\text{O}$.

To determine the affinities of mineralized waters with their surrounding lithologies, the IIRG method (International Institute for Geothermal Research) developed by [34] was used. This classic method is based on six different parameters (A to F), defined for distinguishing water groups based on the geological features of the main reservoir. The parameters are calculated using Equation (1) through Equation (6), the concentration of the major dissolved species (Na^+ , K^+ , Ca^{2+} , Mg^{2+} , Cl^- , SO_4^{2-} and HCO_3^-), and the sum of cations (Σcat) and anions (Σan), expressed in meq.L^{-1} . The values obtained from the six parameters are compared to standard diagrams (α , β , γ , and δ) and their derivatives (1, 2, 3, and 4), which can be useful to indicate the lithological nature of deep reservoirs [34]. To calculate the parameters (A to F), equations were used as follows:

$$A = 100 \times [\text{HCO}_3^- - \text{SO}_4^{2-}] / \Sigma\text{an} \quad (1)$$

$$B = 100 \times [(\text{SO}_4^{2-} / \Sigma\text{an}) - (\text{Na}^+ / \Sigma\text{cat})] \quad (2)$$

$$C = 100 \times [(\text{Na}^+ / \Sigma\text{cat}) - (\text{Cl}^- / \Sigma\text{an})] \quad (3)$$

$$D = 100 \times (\text{Na}^+ - \text{Mg}^{2+}) / \Sigma\text{cat} \quad (4)$$

$$E = 100 \times [(\text{Ca}^{2+} + \text{Mg}^{2+}) / \Sigma\text{cat}] - (\text{HCO}_3^- / \Sigma\text{an}) \quad (5)$$

$$F = 100 \times [(\text{Ca}^{2+} - \text{Na}^+ - \text{K}^+) / \Sigma\text{cat}] \quad (6)$$

The equilibrium reservoir temperatures in this study were estimated by a combination of the following methods:

- The solute geothermometers using the software SOLGEO was used to easily perform calculations of the subsurface temperatures, which was programmed by [35]. In this work, the selected solute geothermometers are based on the concentration of: Na-K, Na-K-Ca, Na-K-Mg, Na-Li, and SiO₂.
- The multi-component geothermometry method [36] is based on the modelling of mineral saturation indexes against temperatures by the PHREEQC speciation software [37]. In these calculations, the standard PHREEQC database (phreeqc.dat) was used. The selected minerals used for estimating the equilibrium temperature were based on the lithological nature of the host rocks present in this region.
- The Na-K-Mg triangular diagram proposed by [38] can be used to evaluate the temperature at which the thermal waters reach the thermodynamic equilibrium with solid phases composed of these elements.

4. Results and Discussion

4.1. Local Geology

The thermal spring of Goutitir is located 20 km west of the town of Taourirt, in the northern part of the Neogene Guercif Basin (Figure 1), north of the foothills of the Koudiet-Zireg anticline. The latter, at an altitude varying between 350 and 500 m, constitutes a sub-circular dome whose limestone strata are oriented E–W. These Jurassic strata are intensely faulted and surrounded by Miocene and Quaternary formations (Figure 2). This dome corresponds to a diapiric structure whose installation is related to Alpine tectonism, precursors of the ascending movements of the underlying Triassic evaporitic clays [24,39]. Near the thermal spring, the Triassic series is often dislocated and incomplete. The formations outcrop there in the form of scales of red clay rich in highly deformed evaporates, highlighting the thrust faults affecting this region (Figure 2). The Jurassic formations, however, present lower Early Jurassic to the upper Kimmeridgian. The Early Jurassic (Toarcian) is composed of dolomitic flint limestones occupying the core of the dome [22,28,40,41]. These formations are in places oxidized, brecciated, and traversed by veinlets of iron oxides, calcite, fluorite, and barite, attesting to a very significant hydrothermal circulation in this region. The southern flank of this dome is materialized by an alternation of micritic limestones a greenish-gray gypsiferous marls, which also outcrop further west of this dome [22,40]. These formations are overlaid by black schistose marls from the Upper Aalenian, outcropping to the north of the dome in the valley of Oued El Abed [15,28,40]. Their schistose appearance, clearly visible in the vicinity of the thermal spring, is probably related to the activity of the major thrust near Oued El Abed. This overlap is highlighted for the first time in this region. The Bajocian is materialized by green and yellowish marls followed by an alternation of marls and limestones [22,28,40]. The Oxfordian, outcropping north of the source of Goutitir, is formed by a sandstone series showing an alternation of yellow sandstone and carbonate sandstone. In the northern part of this region crops out a series of massive limestones and dolomites, belonging to the deposition continued with the Miocene layered discordantly on top of the Jurassic formations. These are composed of blocks of yellowish sandstone alternating with marls. Finally, the continental deposits of the Quaternary complete the sedimentation in this basin and rest in angular unconformity, displaying conglomerates with centimetric fragments of all the previously referred formations.

Regarding magmatic activity, the Jurassic formations are intruded by a swarm of magmatic thickness (0.5 to 4 m). These are alkaline porphyritic lamprophyres with centimetric phenocrysts of biotites and pyroxenes. The dating of these alkaline rocks has yielded, using the K-Ar method [42], ages ranging from the end of the Cretaceous (67 ± 0.2 Ma) to the late Paleocene (57 ± 3 Ma). These lamprophyres locally contain a wide variety of xenoliths, the most important of which are those of syenites, carbonatites, gabbros, and mantle xenoliths [42,43]. Plio-Quaternary magmatism is visible in the region with the installation of volcanic cones, and calc-alkaline and alkaline basaltic lava flows [44].

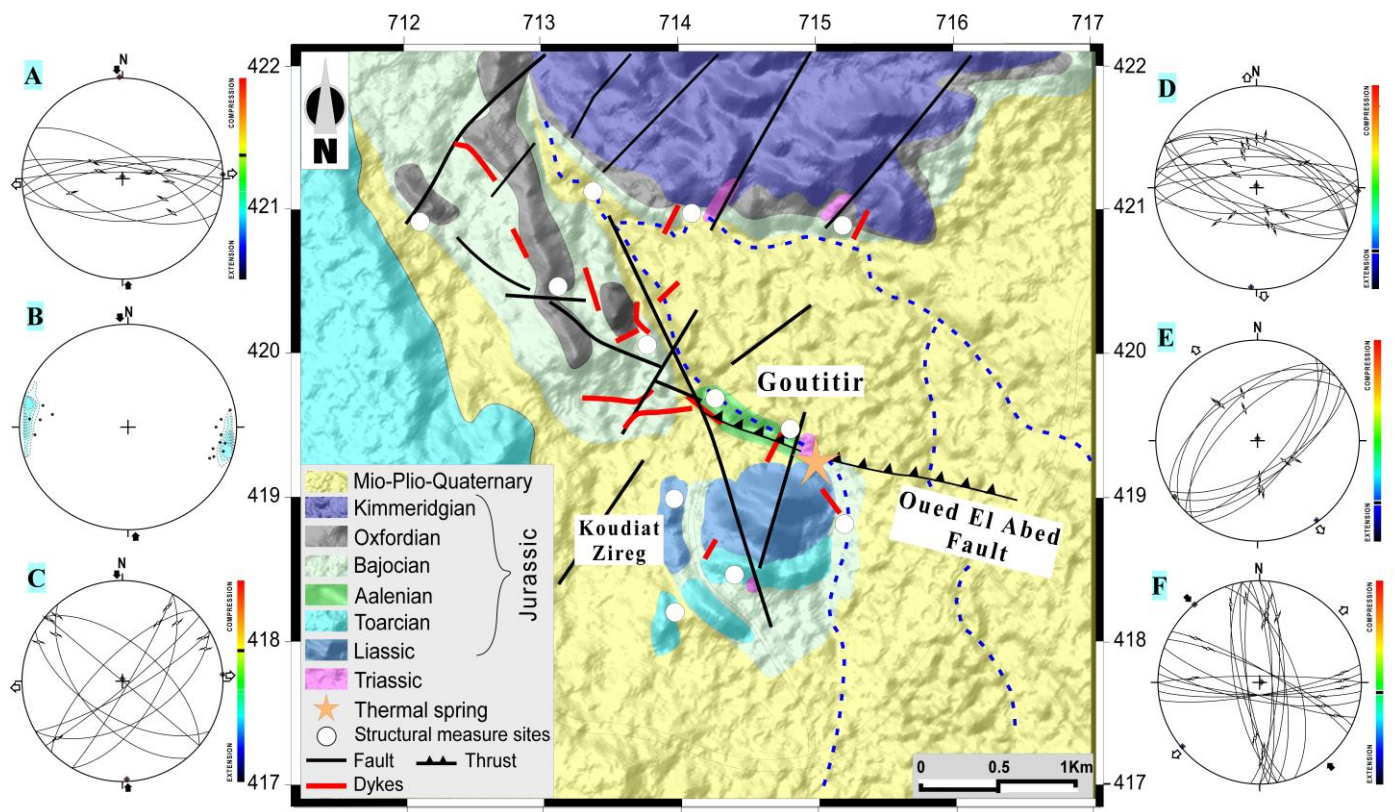


Figure 2. Simplified geological map of the Goutitir thermal spring zone. The stereograms (A–F) represent the different tectonic structures affecting this region.

4.2. Structural Analysis

The Guercif Basin is the eastward extension of the South Rif Thrust. This NE–SW elongated basin was installed at the front of the Rif Belt and was essentially filled by a thick Neogene series [30,45,46]. However, the evolution of the Guercif Basin is largely part of the geodynamic framework of the northern Middle Atlas. Indeed, this basin has been the site of a series of deformation events from the Triassic to the present, namely within the framework of different geodynamic scenarios, such as the opening of the central Atlantic Ocean and western Tethys Ocean, and the collision between the African and Eurasian plates [26,47–49]. These tectonic events are at the origin of the structural architecture of this basin, well marked by ductile and brittle structures reflecting the successive impact of these different deformations. To understand the influence of the different tectonic structures affecting the region of Goutitir, a structural analysis was carried out in the vicinity of this thermal spring. The performed structural measurements allowed the identification of three tectonic phases, which correspond to the final phases recorded in this sector, namely in the following order:

- (a) A first compressive event generated N080–N130 thrusts (Figure 2A). These often evolved into reverse faults and thrusts associated with south-verging folds (Figure 2B). In this sector, the river Oued El Abd corresponds to a N110–N120, 50° N dip fault corridor. This corridor, materialized by a multitude of overlapping faults, has been identified as a major structure associated with this phase (Figure 3A). The analysis of this corridor near the thermal spring of Goutitir shows that it is marked by a “crushing” zone whose thickness varies between 80 and 100 m, where the Triassic red sediments are mixed with Jurassic carbonates and the yellowish Miocene formations. The entire sequence is folded with southern vergence (Figure 3B); as in the case of the Rif Belt, detachments are often observed occurring at the level of the Triassic red clay formations [50,51]. Furthermore, the presence of an anticlinal structure, oriented N120,

in the carbonate formations at the southern front of this thermal spring could also be related to the activity of a thrust associated with this corridor. This phase would also be responsible for the appearance of sinistral faults oriented N025–N060 and their dextral conjugates, oriented N130–150 (Figure 2C). These strike-slips form a fault network that would correspond to the northern extensions of the Southern Middle Atlas Fault (SMAF) (Figure 1). In Jurassic carbonate deposits, rectilinear calcium-filled tension cracks and stylolitic joints are also associated with this phase (Figure 3C). Indeed, these two structures would generate a N–S-oriented compressive setting related to Alpine deformation. The structures generated by this are also identified in this sector by [52]. According to these authors, it would correspond to the last P2/3 and P'2 episodes generated by the progressive and continuous deformation in this sector, during the Miocene. These structures are also found in the Eastern Meseta and are compatible with the major phase of the post-nappe Alpine Orogeny formed by the N–S collision between the African and Eurasian plates [48,49,51,53,54];

- (b) The second phase of deformation is extensive, showing a direction from NW–SE to N–S. It results, in the thermal region of Goutitir, from the activation of two families of normal faults with directions N030–N060 and N080–N120 (Figure 2E,F). The interplay of these two conjugated faults forms horst and graben structures, clearly visible in the Jurassic and Miocene formations (Figure 3D). Indeed, this phase would correspond to a reversal of the previous major phase. This inversion is materialized at the level of certain fault mirrors by the superposition of the streaks of this latter phase. This distensive phase would be similar to those defined in the Goutitir sector [28]. It would have been active from the Tortonian to the Messinian, and would be responsible for the birth and filling of post-nappe sedimentary basin, as is the case in the Goutitir sector [45,46,52];
- (c) The third deformation phase corresponds to a new NW–SE direction compressive phase. It is manifested by the appearance of two networks of conjugate faults. The first, N160–N005, shows sinistral movement, whereas the other, displaying N080–N130 faults, has a dextral movement (Figure 2F).

In general, the architecture generated by the succession of phases highlighted in the Goutitir sector allows us to conclude the following:

- (a) NE–SW direction accidents are the most frequent. The geophysical data [17] attest that these would correspond to the continuities, towards the NE, of the major structures of the Middle Atlas under the Neogene basin of Guercif (Figure 1). The NE–SW accidents observed at Goutitir correspond above all to the continuity of the structures generated by the Central Middle Atlas fault (CMAF) and SMAF (Figure 1). Geological and geophysical data consider these structures as crustal accidents with hybrid sets (shear + extension), deeply rooted in the crust. These accidents controlled, initially, the horst and graben configuration as well as the subsidence of the Neogene Guercif Basin, and then the establishment of Eocene and Mio-Plio-Quaternary volcanism [17,20,45,46,52,55,56];
- (b) E–W faults are also abundant, especially in the eastern part of the Guercif Basin. They constitute tectonic structures most often corresponding to large shear and thrust zones that affected the foremost Rif Belt, in particular the Guercif Basin [26,45]. Indeed, it is a system of accidents frequently marked by injections of Triassic evaporates, which can sometimes evolve into anticlinal structures caused by salt domes. This case was described near the thermal spring of Goutitir. The rise of Triassic salt deposits through the Mesocenozoic sequences leads to the conclusion that the rooting of these accidents is also very deep. According to the estimate made by gravimetric and aeromagnetic methods, these faults could reach depths of up to 3.5 km [17]. These depths would exceed the upper limits estimated, in this basin, for the Paleozoic basement [46]. Thus, these faults would also be structures anchored in the Paleozoic basement, reactivated during the late Alpine phases;
- (c) N–S structures are rare in the Goutitir area. They are localized, appearing only in the eastern part, near Wadi Abd. Geophysical data confirm that these faults are

interpreted as superficial accidents that do not reach the Paleozoic basement [17,55]. They would probably be generated during the Alpine orogeny by the convergence of the African and Eurasian lithospheric plates [49].

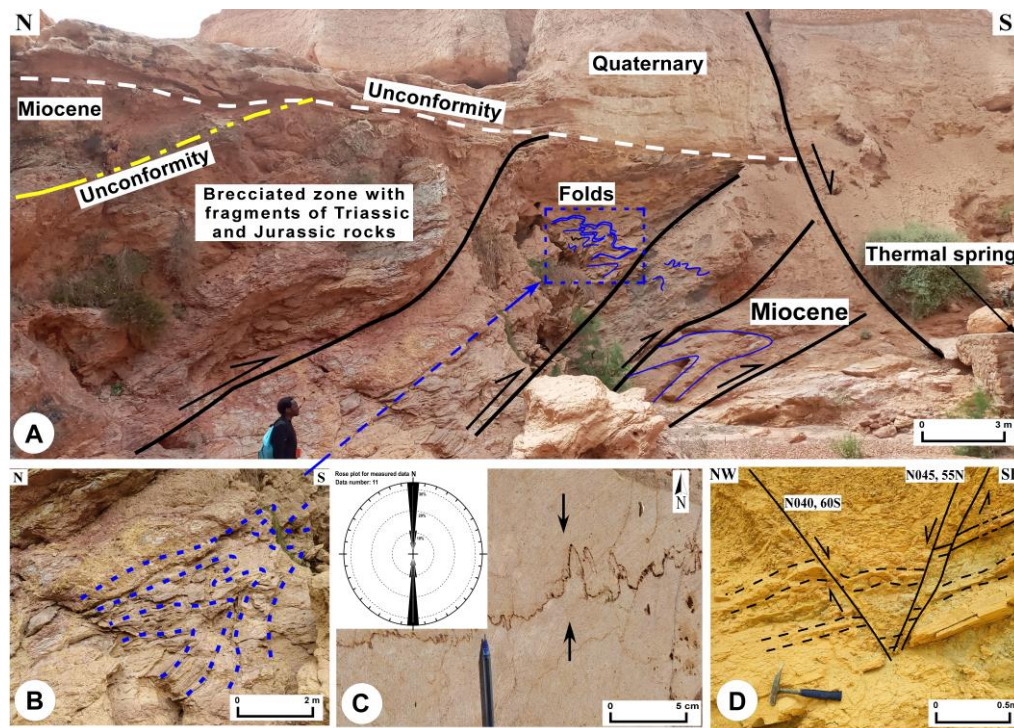


Figure 3. (A) Structures associated with the E–W thrust at Wadi El Abd, in the vicinity of the thermal spring of Goutitir; (B) folds associated with this overlap; (C) stylolites outcropping in limestones associated with the compression phase; (D) horst and graben structure. The arrows show the movement of the faults.

4.3. Physico-Chemical Composition

The physico-chemical composition of the Goutitir water sampled in 2019 is very similar to the compositions reported by [5,14–16] (Table 1). Over 20 years the temperature, mineralization, and composition have limited variation. Indeed, the emergence temperature varies from 42.5 to 44.5 °C, and the pH varies between 6.2 and 7.3, with an average of 6.7, attesting to the slightly acidic to neutral nature of this water. The Total Dissolved Solids (TDS) and Electric Conductivity (EC) vary from 8.79 to 10.48 g/L (Figure 4) and 13.78 to 15.58 mS/cm, respectively, indicating very high salinity. The composition of the major dissolved species plotted on the Durov diagram [57] attests to their sodium-chloride hydrochemical facies (Figure 4), despite the high sulphate and calcium concentrations. The sodium and chloride concentrations varied from 2100 to 2582 mg/L and from 3600 to 4375 mg/L, respectively. While the dissolved sulphate and calcium have values between 1970 and 2500 mg/L, and 691 and 950 mg/L, respectively. The bicarbonate content does not exceed 250 mg/L.

The variation in the chemical composition of these waters can be depicted in the Schöeller–Berkaloff diagram (Figure 5), where these waters display great similarity, despite the variability of the Mg^{2+} and HCO_3^- concentration. These patterns are characterized by high contents of Cl^- and Na^+ , confirming the hydrochemical facies of Na-Cl type, as well as $Ca-SO_4^{2-}$.

Table 1. Physico-chemical results of the thermal waters of Goutitir along 19 years.

Sample ID	References	Temperature	pH	Total Dissolved Solids	Electric Conductivity	Ca ²⁺	Mg ²⁺	Na ⁺	K ⁺	HCO ₃ ⁻	SO ₄ ²⁻	Cl ⁻	SiO ₂	Sr	δ ¹⁸ O	δ ² H
		°C		g/L	mS/cm	mg/L	mg/L	mg/L	mg/L	mg/L	mg/L	mg/L	(mg/L)	(mg/L)	(‰)	(‰)
G-1	[14]	44	6.7	8.79	14.80	780	174	2100	30	250	1970	3600	32	14		
G-2	[15]	45	7.3	9.77	13.78	870	203	2122	27	244	2160	3994			-8.7	-58.6
G-3	[5]	43.2	6.6	10.48	14.99	950	280	2130	26	204	2500	4375			-8.4	-54.3
G-4	[16]	42.4	6.6	10.12	15.58	865	246	2562	33	192.2	2108	4116				
G-5	This work	44.5	6.2	9.5	14.54	691	150	2380	42	149	2000	4100	35	17	-8.3	-56.5

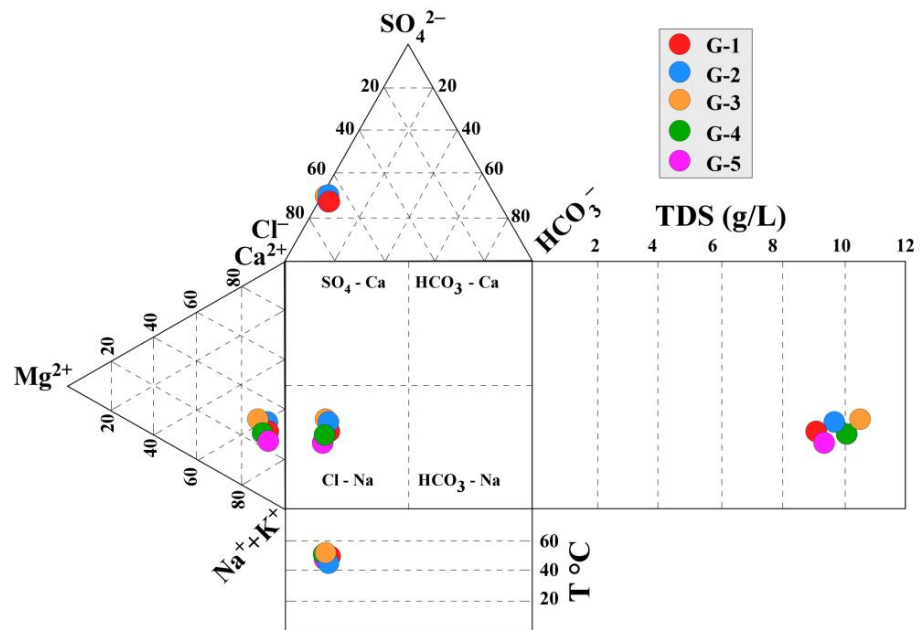


Figure 4. Durov diagram applied to the thermal waters of Goutitir, reported for a different date and from different authors (G1-[14]; G2-[15]; G3-[5]; G4-[16]; G5-this work, 2019).

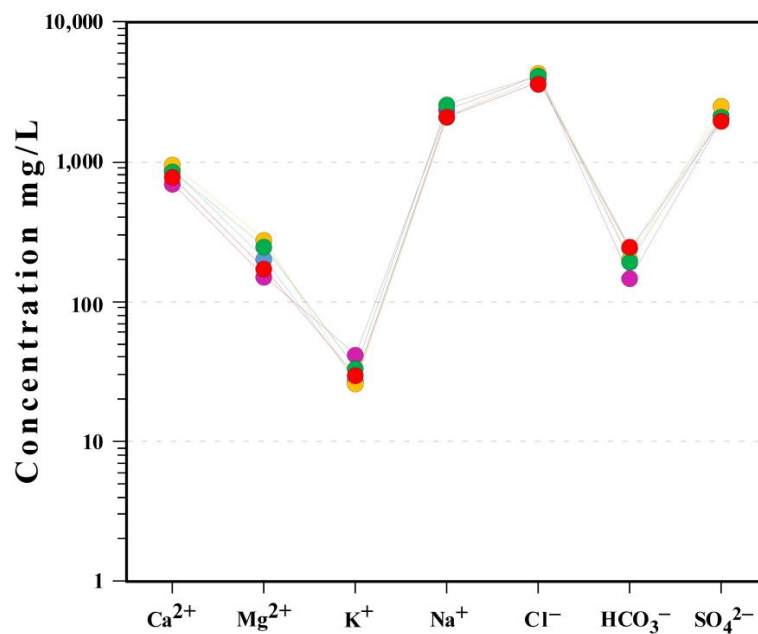


Figure 5. Schöeller-Berkaloff diagram applied to the thermal waters of Goutitir, reported for a different date and from different authors ([5,14–16] (symbols as in Figure 4)).

Considering the high degree of mineralization and the chemical composition of the Goutitir, we can advance the hypothesis that these waters circulate in aquifers very rich in halite and gypsum, probably within the salt from Triassic evaporitic formations in the area (Figure 2). Furthermore, these waters are characterized by moderately high levels of Ca^{2+} , Mg^{2+} , and HCO_3^- , attesting that during their circulation at depth and their transfer to the surface, these waters have interacted with carbonate rocks, namely Jurassic carbonate (limestone and dolomite), or Ca-rich basic magmatic rocks (with plagioclase and/or clinopyroxene). These waters also contain relatively high K^+ concentrations (26–42.1 mg/L) compared to other thermal waters of eastern Morocco, where K^+ values rarely exceed 13 mg/L [5,14]. This value for the thermal waters of Goutitir probably implies the interaction of these waters with silicate minerals that can provide this element, such as biotite or K-feldspar. In this region, in addition to the Paleozoic basement intruded by granitoids ~10 km from Goutitir, a swarm of lamprophyric veins outcrop in the vicinity of this source. Both biotite and K-feldspar are part of the primary mineral assemblage of these veins [42]. Near this source, these veins become friable and altered, revealing a centimetric biotite of probable hydrothermal origin. However, this element may also be derived from sylvite, which is absent in the Triassic formations of the Atlas domain [58], but detected in the fluid inclusions of the fluorite ores of Tirremi located 10 km north of the Goutitir thermal spring [59].

The high levels of Sr (17 mg/L) and Br (2.80 mg/L) would probably be linked to the interaction of these waters with the evaporitic formations of the Triassic and carbonated formations of the Jurassic. These deposits, which outcrop in this sector, would be able to supply Br from bromite, which is often present in evaporitic deposits, and Sr via strontianite from carbonate deposits [13], or from the plagioclases of the magmatic rocks present in this region [42]. The equally high contents of SiO_2 (32 to 35 mg/L) would be related to the interaction of these waters with the crystalline basement of the eastern Meseta composed of schisto-greaseous rocks and felsitic granitoids of Hercynian age.

Geothermal waters that emerge at the surface with minimal contamination by ground-water or volcanic water are considered by Giggenbach (1988) as mature waters (Figure 6). These waters are generally in equilibrium with the reservoir rocks of which they carry the chemical signature and have a chloride concentration higher than that of bicarbonate and sulfate, differentiating them from immature waters largely influenced by cold surface waters. On the Cl^- - SO_4^{2-} - HCO_3^- ternary diagram [12], which differentiates the mixing process between deep mature thermomineral waters and cold surface waters, the waters of Goutitir show an enrichment in SO_4 placing them in the domain of waters that have evolved in hydro-volcanic systems (Figure 6). However, based on the geological context of Goutitir, the SO_4 enrichment could originate during the upward transfer of these waters to the surface, as is the case in the thermal springs of central [60] and eastern Turkey [61], which would be from the following:

- (i) The oxidation of H_2S derived from cooling magma in Quaternary volcanoes located near this spring. They would thus be the origin of SO_4 ions by the reaction $\text{H}_2\text{S} + 4\text{H}_2\text{O} \rightarrow \text{SO}_4^{2-} + 10\text{H}^+$; the deep circulation of these fluids through the volcanic rocks are probably the sources of the lamprophyric veins that outcrop in abundance in this region. The circulation and transfer of these waters to the surface would probably have followed the same tectonic discontinuities that favored the establishment of the lamprophyre swarm. This would certainly have allowed these waters to remain in contact with these rocks for a long period;
- (ii) The reactions of these waters with the sulphide mineralizations present in the basement of this basin [59], allowing their dissolution. These reactions would provide SO_4 as, for example, the oxidation of pyrite, according to the reaction $2\text{FeS}_2 + 7\text{O}_2 + 2\text{H}_2\text{O} \rightarrow 2\text{Fe}^{2+} + 4\text{SO}_4^{2-} + 4\text{H}^+$;
- (iii) The interaction of these waters with the gypsum-rich Triassic evaporitic clay and Miocene marl formations.

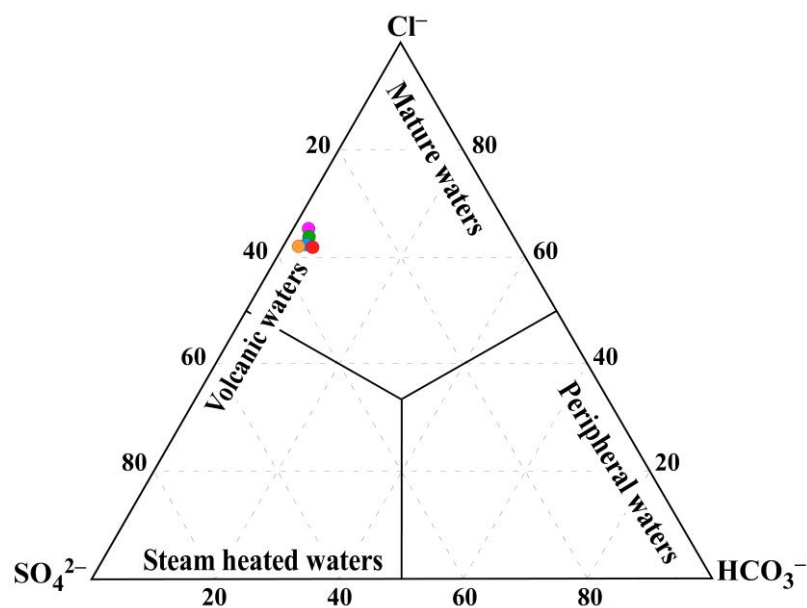


Figure 6. Triangular Cl^- – SO_4^{2-} – HCO_3^- diagram of [12] applied to the thermal waters of Goutitir, reported for a different date and from different authors ([5,14–16]; this work, 2019), (symbols as in Figure 4).

The elements in minor concentrations can constitute very good markers to retrace the history of the thermal waters. They make it possible to identify the different interaction processes between these waters and the different rocks of the reservoirs crossed. Only the trace elements carried out in this work have been treated (Table 2).

Table 2. Minor and trace elements dissolved in the thermal waters of (This work 2019), Oulmès and Ain Allah [14].

		Goutitir (G5)	Oulmès	Ain Allah
	Reference	This work	[14]	[14]
Li	($\mu\text{g/L}$)	579	4900	12
Br	($\mu\text{g/L}$)	2800	1800	6000
Be	($\mu\text{g/L}$)	1	100	0.1
F	($\mu\text{g/L}$)	2600	1200	0.1
Sc	($\mu\text{g/L}$)	10	-	-
Ti	($\mu\text{g/L}$)	1	-	-
V	($\mu\text{g/L}$)	1	-	-
Mn	($\mu\text{g/L}$)	3.6	1280	2
Cr	($\mu\text{g/L}$)	5	-	-
Co	($\mu\text{g/L}$)	0.074	0.1	0.1
Ni	($\mu\text{g/L}$)	3.1	1	1
Cu	($\mu\text{g/L}$)	19.8	0.3	0.4
Zn	($\mu\text{g/L}$)	46.5	17	190
Ga	($\mu\text{g/L}$)	0.1	-	-
Rb	($\mu\text{g/L}$)	152	310	16
Y	($\mu\text{g/L}$)	0.088	-	-
Nb	($\mu\text{g/L}$)	0.05	-	-
Mo	($\mu\text{g/L}$)	4.7	-	-
Cd	($\mu\text{g/L}$)	0.1	0.1	0.1
Sb	($\mu\text{g/L}$)	0.24	-	-
Cs	($\mu\text{g/L}$)	66.5	200	4
Ba	($\mu\text{g/L}$)	35	380	21
W	($\mu\text{g/L}$)	1.61	-	-

Table 2. Cont.

		Goutitir (G5)	Oulmès	Ain Allah
Tl	($\mu\text{g/L}$)	1.36	-	-
Pb	($\mu\text{g/L}$)	1.09	0.1	0.1
Bi	($\mu\text{g/L}$)	3	-	-
Th	($\mu\text{g/L}$)	0.055	-	-
U	($\mu\text{g/L}$)	0.574	-	-
In	($\mu\text{g/L}$)	0.01	-	-
Zr	($\mu\text{g/L}$)	0.1	-	-
Hf	($\mu\text{g/L}$)	0.01	-	-
Al	($\mu\text{g/L}$)	31	50	30
Fe	($\mu\text{g/L}$)	100	16,000	47

The elements in minor concentrations in the Goutitir thermal water are represented in the form of patterns normalized to the chondrites [62] in the logarithmic diagram (Figure 7A). The elements Li, Rb, Cs, Ba, and U show contents of 579 $\mu\text{g/L}$, 152 $\mu\text{g/L}$, 66.5 $\mu\text{g/L}$, 35 $\mu\text{g/L}$, and 0.547 $\mu\text{g/L}$, respectively (Table 2). These values are marked for Li, Rb, Cs, and U by the positive anomalies observed (Figure 7A), implying the circulation of these waters through the crystalline basement (magmatic and metamorphic rocks). Indeed, these elements may originate from the dissolution of silicate minerals (K-feldspar and mica) composing the felsic igneous rocks [13,63].

The high levels of F (2600 $\mu\text{g/L}$) and moderate levels of Fe (100 $\mu\text{g/L}$), Ba (35 $\mu\text{g/L}$), Zn (46.5 $\mu\text{g/L}$), Cu (19.8 $\mu\text{g/L}$), Pb (1.1 $\mu\text{g/L}$), and W (1.61 $\mu\text{g/L}$) can be linked to the interaction of these waters with the mineral deposits present in this area. In fact, the Jurassic and Paleozoic basement abound in mineral occurrences spread over an area of 900 km^2 , including the entire Goutitir sector [59]. On the spider diagrams, the positive anomaly displayed by Pb would be related to the interaction of these waters with sulfides (Galena PbS) mined in Jurassic limestones with barite, fluorite, Cu, and Fe-Mn oxide sulfides associated with silica and calcite veins in the Jbel Tirremi mine, located ~10 km NE of this source [22,59]. In addition, the origin of Ba may also come from K-feldspars in magmatic rocks of the Paleozoic basement hosting granites and probably syenites present as xenoliths in the lamprophyres. This implies that these waters must also have circulated through the same pathways as the mineralizing fluids.

The concentrations of transition elements, notably Cr (5 $\mu\text{g/L}$), Ni (3.1 $\mu\text{g/L}$), and Sc (10 $\mu\text{g/L}$), are probably related to the interaction of these waters with basic and ultrabasic rocks. In fact, these rocks are susceptible to provide these elements during the interaction of these waters with the minerals carrying these elements such as spinels, clinopyroxenes, and to a lesser degree, amphiboles [64–66]. In lamprophyre dykes and sills, gabbro and pyroxenite xenoliths have been described [42], providing evidence for the existence of basic and ultrabasic garnet deposits at depth in the basement of the Neogene Guercif basin.

Moreover, the high Sr, marked in these patterns by a positive anomaly, would be related to the interaction of these waters with the plagioclases of the magmatic rocks of the basement and the calcite of the overlying Jurassic carbonate formations.

In the diagram (Figure 7B), the patterns of the thermal waters of Goutitir are compared with other thermal springs rising in the different structural areas of Morocco: with those of Oulmès, which springs in the Paleozoic granites of the western meseta; and those of Ain Allah, which rises in the Miocene marls of the South Rifain Sillon, and whose waters are pumped directly from the Liassic reservoir. The pattern of Goutitir is slightly less enriched and shows a parallelism with that of Oulmes compared to that of Ain Allah. The similar anomalies between these two patterns, notably those of Rb and Cs, attest once again that the waters of Goutitir have circulated in the Paleozoic basement. However, their enrichment in Ni, Cu, and Pb would be, respectively, related to the circulation of these waters within the basic and ultrabasic rocks and within the mineralized deposits characterizing the basement of this region. This comparison indicates the circulation of

these waters in the basement such as Oulmès, with additional arguments which attest to their circulation in magmatic rocks.

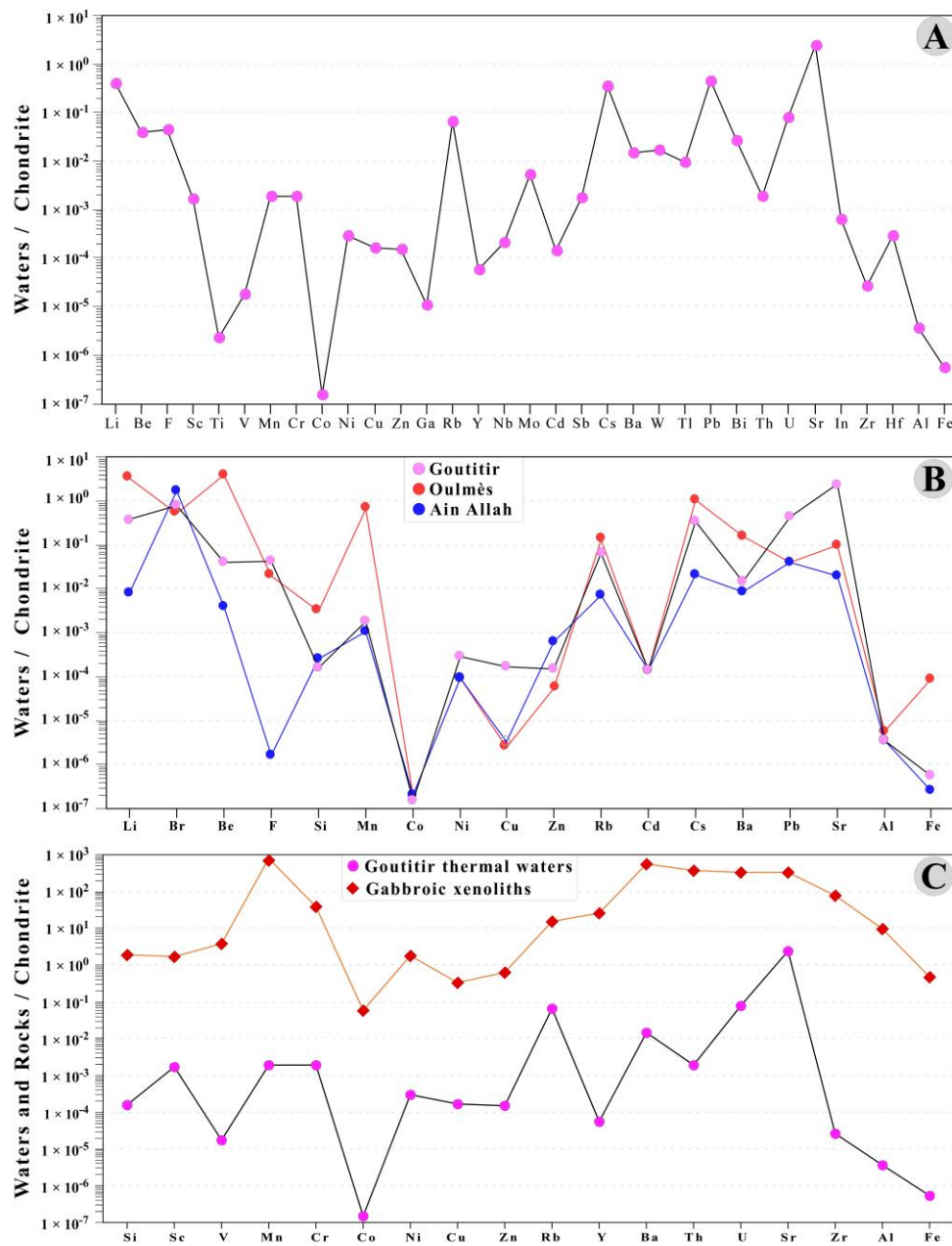


Figure 7. Chondrite-normalized trace elements patterns for the Goutitir thermal waters (A); Goutitir, Oulmès, Ain Alah thermal waters (B); and Goutitir thermal waters and Gabbro (C).

4.4. Affinity between Water and Reservoir Rock Compositions

The affinity of mineralized waters with the reservoir lithology can be highlighted using the D’Amore approach [34]. Applied to the Goutitir thermal water samples, this approach shows that the patterns of these thermal waters show a pattern comparable to the standard pattern of type (2) of [34], which characterizes sodium and potassium chlorinated waters. This type of pattern also characterizes thermal waters that have deep circulation through mafic volcanic rocks. The variations observed in parameters A (Equation (1)) and F (Equation (6)) (Figure 8) show a slight decrease compared to the reference value (A and F ≈ 0). These slight variations can be explained by the circulation of these waters through evaporitic formations of the Triassic and Miocene, reflected by an increase in the

contents of Na^+ and SO_4^{2-} . Moreover, this result seems more plausible if one also considers the large magmatic outcrops in the region, namely Eocene alkaline lamprophyric veins and Quaternary calc-alkaline and alkaline magmatism. Many xenoliths of alkaline pyroxenites, gabbros, nepheline syenites, and calcic carbonatites have been described in lamprophyric veins [42]. These granular xenoliths confirm the existence at the depth of mafic to ultramafic batholiths. This corroborates the deep circulation of Goutitir waters within the basic and ultrabasic magmatic formations. As previously referred to, the interaction of the Goutitir thermo-mineral waters with these rocks is also suggested by their trace element content. However, the reference pattern indicates that these waters indeed circulated in mafic rocks of an ophiolitic nature. Nevertheless, the existence of mafic igneous rocks of ophiolitic nature in eastern Morocco is still debatable.

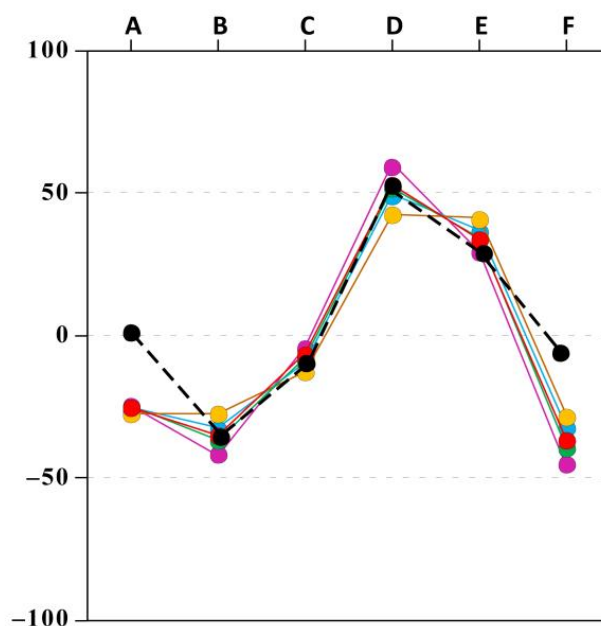


Figure 8. Application of the IIRG method [34] to the thermal waters of Goutitir; (symbols as in Figure 4 and the reference pattern is black).

4.5. Aqueous Geothermometry

The temperature of the geothermal reservoir can be estimated by different geothermometric methods. During its transfer to the surface, the thermal water can undergo mixing with colder waters, generally accompanied by a decrease in temperature and a change in mineralization. This generally obliterates their geochemical history and complicates the use of chemical geothermometers, leading either to a temperature overestimation or underestimation. Geothermometers assume that there is no significant chemical change in the water during its ascent [67]. However, thermal waters, such as those from Goutitir, are likely to preserve their geochemical signatures from the reservoirs they crossed during their transfer to the surface [12]. Five aqueous geothermometers, based on the concentrations of the major dissolved species (Na-K, Na-K-Ca, N-K-Mg, Na-Li, and SiO_2) were chosen to estimate the equilibrium temperatures of these waters in the reservoir. The application of the different geothermometers for these waters provides estimated temperatures varying between 87 °C and 124 °C (Table 3). These values, significantly higher than the measured temperatures, imply a temperature dissipation of 41.5–79.5 °C during the water flow, from the reservoir to the surface. This dissipation could be due either to thermal diffusion along the faults used by these waters to ascend to the surface, or mixing with water from the overlying aquifers.

Table 3. Deep reservoir temperatures estimated by aqueous geothermometers (°C).

T (°C)	Geothermometer
103	Na-K geothermometer [68]
124	Na-K geothermometer [38]
94	Na-K geothermometer [69]
110	Na-K geothermometer [70]
114	Na-K-Ca geothermometer [71]
99	Na-K-Mg geothermometer [72]
89	Na-Li geothermometer [73]
124	Na-Li geothermometer [70]
86	SiO ₂ geothermometer [68]
87	SiO ₂ geothermometer [70]

In the triangular diagram K-Na-Mg^{1/2} of [38] (Figure 9), the thermal waters of Goutitir do not show any influence of dilution by colder waters, but they are near the Mg pole. This could be explained by their interaction with dolomitic limestones within liasic reservoirs rich in this element or from ferromagnesian minerals of basic and ultrabasic magmatic rocks of the basement. In addition, the position of the waters in Figure 9 is consistent with equilibrium temperature estimates of 90–110 °C, which is quite similar to the obtained results using the above aqueous geothermometers.

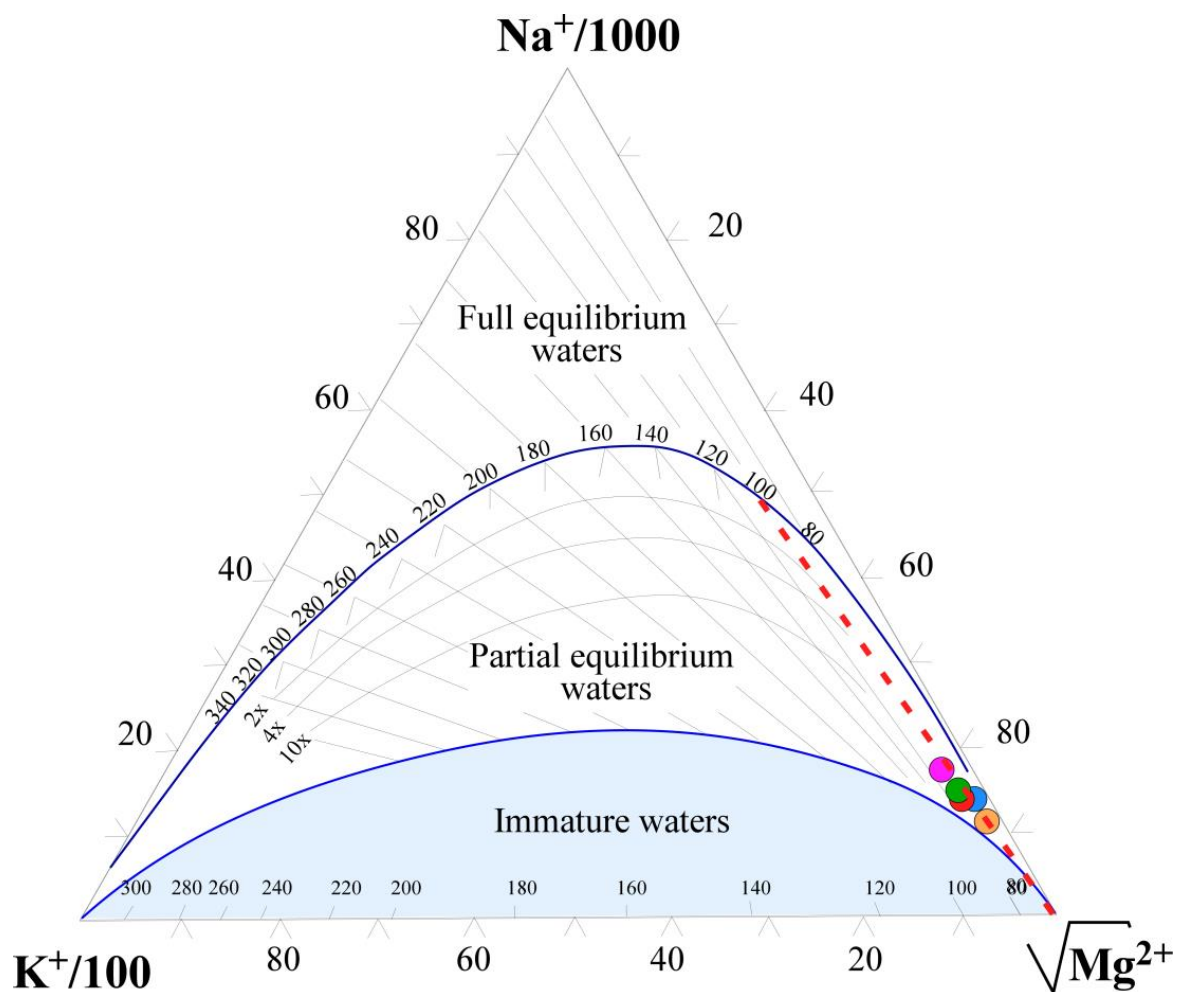


Figure 9. Na-K-Mg^{1/2} diagram applied to the thermomineral waters of Goutitir (after [38]). Symbols as in Figure 4, red dash line indicate the equilibrium temperature.

In order to confirm the reservoir temperature estimated by the previous methods, an approach of multi-component geothermometry [36], based on the thermodynamic equilibrium of the water related to the most likely solid phases in the reservoir, was used. The equilibrium was calculated through the saturation indexes (SI) of water for the temperature range of 30–210 °C while adopting a mineralogy based on the geological context of the basement and its cover (Figure 10).

This mineralogical assemblage shows that the waters of Goutitir have, during their transfer to the surface, been equilibrated in geothermal reservoirs of different lithological nature. It is initially a metaluminous reservoir composed by metamorphic rocks from pelitic origin. This reservoir would be, respectively, at the origin of gibbsite, muscovite and kaolinite at temperatures between 100 and 115 °C. These waters will then begin their re-equilibration within the same reservoir replete with basic and ultrabasic magmatic rocks (gabbro, syenite, and pyroxenites) at the origin of chromite from gabbros and pyroxenites as well as clay minerals from metaluminous metamorphic rocks (gneiss, micaschist, etc.) and feldspars from syenites at temperatures around 95 °C. These waters will then migrate to the overlying Liassic reservoir intruded by alkaline lamprophyres (microsyenitic). where they will undergo their final re-equilibration before their transfer to the surface. In this reservoir, the re-equilibration would involve carbonate minerals (aragonite, calcite, and dolomite) from the liasic dolomitic limestones and potassium feldspars originating from the microsyenitic lamprophyres at temperatures around 75 °C. These minerals attest that the circulation of these waters occurred in the basement within the basic and ultrabasic magmatic rocks, in the crystallophyll basement, and in the overlying carbonate and evaporitic clay formations.

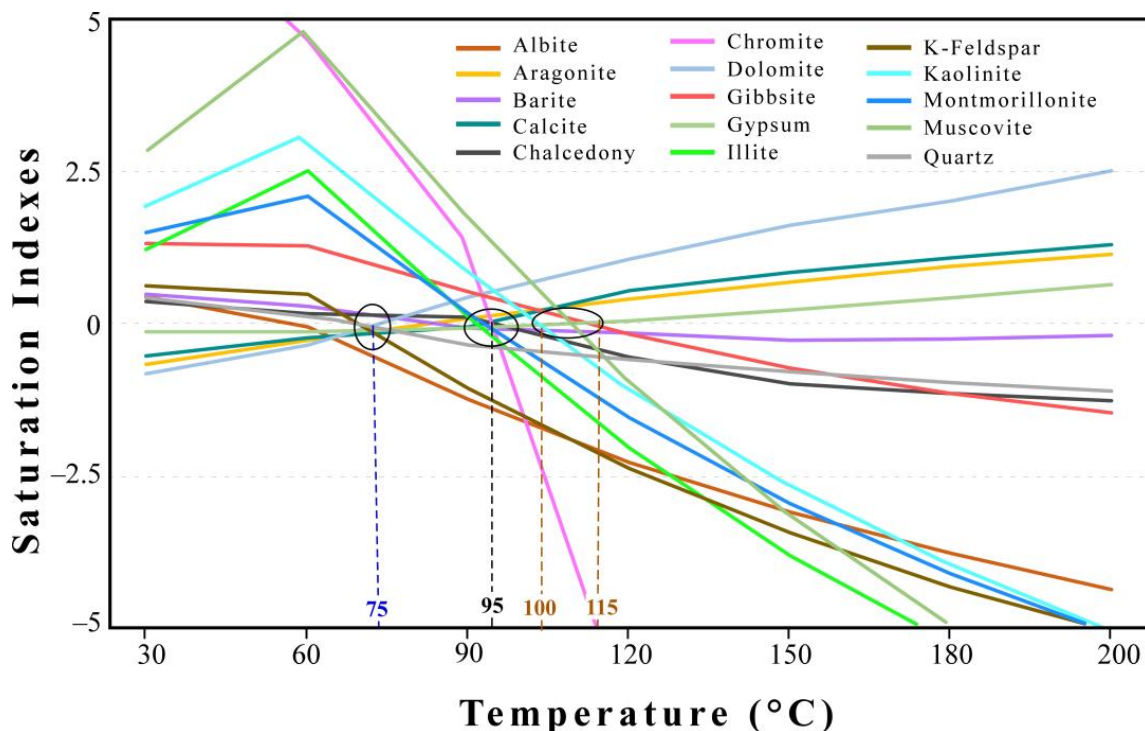


Figure 10. Saturation indexes (in log(Q/K)) of the thermal water Goutitir in different minerals and temperatures.

Considering the estimated geothermometric temperatures (80–110 °C) for the Goutitir water reservoir, the air temperature in the recharge area of about 20 °C, and the geothermal gradient established for this region, which is ~35 °C/km [3,9], the Goutitir water reservoir can be located at depths between 2 and 3.5 km. Indeed, these depths would correspond, according to the drilling data (TAF1X) and the seismic data established in the vicinity of the thermal spring of Goutitir in the Neogene basin of Guercif [46,56], to the deepest Paleozoic

crystalline basement reservoirs, located at ~3.5 km, and to the overlying Triassic evaporite and Jurassic carbonate reservoirs, located at a depth of ~2 km.

The geochemical signature of these waters implies their interaction with these various reservoirs during their circulation at depth within a basement where granitic magmatic rocks dominated at this locality by basic and ultrabasic magmatic rocks are emplaced, as well as their interaction with the waters of the overlying evaporitic and carbonated reservoirs.

4.6. Oxygen and Deuterium Isotopes

Stable isotopes (oxygen $\delta^{18}\text{O}$ and deuterium, $\delta^2\text{H}$) are widely used as effective tracers to determine the origins, water–rock interactions, and recharge zones of thermomineral waters. The $\delta^{18}\text{O}$ and $\delta^2\text{H}$ values for the thermomineral waters sampled in this study are shown in Table 1 and are between -8.7 to -8.35‰ (V-SMOW) for $\delta^{18}\text{O}$ and -58.6 to -54.3‰ (V-SMOW) for $\delta^2\text{H}$, respectively. As can be seen on the $\delta^{18}\text{O}$ vs. $\delta^2\text{H}$ diagram (Figure 11A), these values are aligned with the Global Meteoric Water Line (GMWL, $\delta^2\text{H} = 8\delta^{18}\text{O} + 10$; [74]), as well as the line that represents the local meteoric precipitation of Morocco (MMWL, $\delta^2\text{H} = 8\delta^{18}\text{O} + 14$; [75–77]). Thus, these isotopic signatures testify to the meteoric origin of the studied waters. Moreover, their positioning between the GMWL and MMWL suggests that these waters were not subjected to significant surface evaporation. The water–rock interaction, also, did not strongly modify the O isotopic composition (Figure 11A), since the positive shift of the $\delta^{18}\text{O}$ (considering the MMWL) is only of 0.30‰ (G-2), 0.11‰ (G-3), and 0.46‰ (G-5).

Since the isotopic composition of these waters was not strongly modified, it is possible to use the isotopic data to estimate recharge altitudes, which is applicable only for recent waters (Holocene recharge) that have not undergone a paleoclimatic effect.

Since the $\delta^{18}\text{O}$ isotopic values in the Goutitir vary between -8.7 and -8.35‰ , it is suggested that the recharge zone is characterized by a very cold climate where evaporation processes are very limited. According to [78], the $\delta^{18}\text{O}$ isotopic depletion gradient for the Rif and the Middle Atlas groundwater is about $\sim 0.25\text{‰}$ per 100 m ASL. Using the isotope data obtained by these authors for the water from wells in the Rift and Middle Atlas regions (Figure 11B), the recharge zone of Goutitir waters would be located at an altitude between 1890 and 2008 m ASL if we consider the $\delta^{18}\text{O}$ water content or 1820 and 1920 m ASL if we use the $\delta^2\text{H}$ values (Figure 11C).

These altitudes can be observed southeast of the thermal spring of Goutitir, namely in the Middle Atlas belt, where mountainous ridges well above 2000 m are common (Tichoukt, Bou Iblane, Bounacer, etc.). This suggests that the recharge areas of these waters would be located southwest of Goutitir in the mountainous reliefs of the anticlinal ridges shaped by the major accidents traversing the Middle Atlas. Geophysical studies [17,45,46,56] show that SMAF extends towards the northeast under the Neogene cover of the Guercif basin as a NE–SW fault network reaching the Goutitir region (Figure 1). Thus, this lithospheric accident would have facilitated the infiltration and circulation of meteoric waters to depth. It would also have served as a lateral conduit for these waters from the southwest high altitudes of the Middle Atlas to the northeast in the Goutitir area.

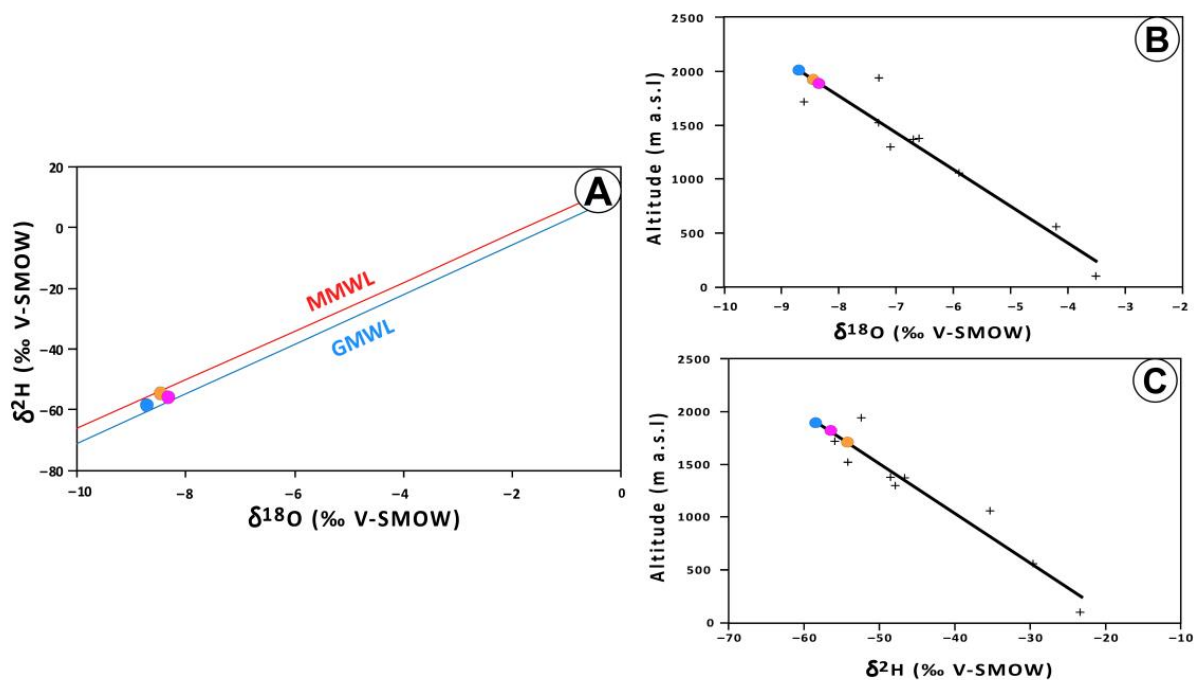


Figure 11. Diagrams (A) $\delta^{18}\text{O}$ vs. $\delta^2\text{H}$ for the samples of the waters collected in the northeast of Morocco. GMWL—Global Meteoric Water Line; MMWL—Moroccan Meteoric Water Line, (B) altitude vs. $\delta^{18}\text{O}$ and (C) altitude vs. $\delta^2\text{H}$ for Goutitir thermal waters. (Symbols as in Figure 4).

The total dissolved carbon in waters can have both an organic and inorganic origin. When associated with the dissolution of organic matter, it has average of $\delta^{13}\text{C}$ values between -26 and -20‰ vs. V-PDB [79]. Carbon of inorganic origin can result from the following: (i) the dissolution of carbonate rocks, or from thermometamorphic reactions, presenting $\delta^{13}\text{C}$ values of $0 \pm 2\text{‰}$; (ii) a mantle origin, or from the degassing of magmas, with $\delta^{13}\text{C}$ values ranging between -3 and -5‰ in the most primitive fluids [80]. According to [78], the Goutitir water contents of $\delta^{13}\text{C}$ are -5.1‰ , and this value allows the estimation that 60% of the dissolved C comes from the dissolution of carbonate rocks (or from thermometamorphic reactions), falling into the field defined by [78] as representative of carbonate dissolved waters of the Lias in Morocco (with a total dissolved inorganic carbon lower than 500 mg/L). This value ($\delta^{13}\text{C} = -5.1\text{‰}$) is close to that of magma degassing ($\delta^{13}\text{C}$ between -3 and -5‰), also suggesting the provenance of carbon from degassing in primitive fluids associated with Quaternary volcanism represented by many of the edifices that outcrop in this region.

The apparent age of this water, based on the ^{14}C content (5.7 ± 0.5 pCm) [78], is estimated between 9000 and 14,500 yBP. Since the $\delta^{18}\text{O}$ composition does not seem to reflect a long water–rock interaction, it is possible that this water contacts and dissolves other rocks in depth, where the oxygen content is not significant or the dissolution temperature is not very high.

4.7. Hydrogeological Conceptual Model

The thermal spring of Goutitir is located within the Neogene formations of the Guercif Basin. The structural architecture of this basin was shaped by the Alpine Orogeny, which allowed the reactivation of the NE–SW, E–W, and N–S fault structures. The dominance of NE–SW structures in this sector probably played a major role in the establishment of the thermal discharge in this thermal spring. Indeed, this resurgence is located at the intersection of two important NE–SW and E–W faults. The E–W thrusts are composed of layers of low-permeability Triassic clayey formations, implying that these thrusts correspond to detachments occurring at the level of the Triassic formations, as is the case in the Rif Belt [50,51].

In addition, the isotopic results confirm that the water discharged by this spring has a meteoric origin, and was probably recharged at an altitude around 2000 m. These altitudes are absent in the Rif mountains and the Middle Atlas located northeast of the Guercif Basin (Figure 1). On the other hand, they can be found in the Middle Atlas located southwest of this basin, being connected by large-scale NE–SW lithospheric accidents, such as the SMAF and CMAF that intersect the entire Middle Atlas. The shaping of this sector by these structures would have played a role not only in the establishment of the abundant volcanic activity known in this sector but also in the hydrothermal activity manifested by the Goutitir thermal spring. These faults represent areas of weakness that contributed to an increase in permeability and fracture/pore connectivity in the rocks, facilitating the infiltration and circulation of groundwater at different depths while forming a preferential pathway between the different reservoirs. Since the recharge altitudes are located in the southeast, this NE–SW fault network would facilitate the infiltration and drainage of these fluids towards the Guercif Basin under the Neogene cover, as highlighted by the geophysical data [17,46,56]. In Goutitir, intersection with the E–W thrusts would provide upwelling of these fluids by the low permeability Triassic argillaceous detachment formations inserted in this thrust. Indeed, the significant frequency of major NE–SW and E–W accidents and their relationship in the field with the thermal waters of Goutitir would argue in favor of an established genetic relationship between this source and these structures. The genetic relationship with these two structures, as well as the geometry of the faults at the outcrop, would be connected to a network of very deep faults likely to shape preferential and natural conduits which would facilitate the circulation of hydrothermal fluids at depth and their transfer to the surface. These structures controlled the evolution of the geothermal system in the Guercif Basin and were inherited from ancient variscan structures, which were most likely reactivated as a consequence of the N–S compression associated with the Africa–Europe convergence during the Alpine Orogeny.

The particular geochemical signature of the waters of Goutitir, whose temporal variations are very limited, has remained constant over a period of 19 years. The chemical composition of these waters attests that they probably began their circulation at an estimated depth of 3.5 km within the crystalline basement through basic and ultrabasic plutonic rocks, which constitute the basement of the Guercif Basin. The signature of these rocks on the geochemistry of Goutitir thermomineral waters is reflected on the multi-element diagram comparing the pattern of the trace element contents of the thermal waters with the gabbroic xenoliths inserted in the lamprophyres. These patterns display identical anomalies and almost perfect parallelism, confirming that these thermal waters indeed reacted with these rocks at depth (Figure 7C). The circulation of these waters at this depth would have allowed them to reach a water/rock equilibrium visible in their final geochemical signature. The transfer of these waters to the surface implied the intersection of the overlying Triassic and Jurassic reservoirs, at an estimated depth of 2 km, where some dissolution of Triassic evaporites and Jurassic dolomitized limestones probably occurred. These waters also show small contents of metallic elements, probably reflecting an interaction with known metal deposits in the region. The preponderant geochemical signature of these waters reflects equilibrium with basic and ultrabasic rocks of an ophiolitic nature. Apart from the outcrops of lamprophyres and alkaline basalts in this sector, those of an ophiolitic nature are absent. However, layers of mafic to ultramafic rocks have been described as ophiolites and dated to 190 Ma at the junction between the Mesorif and the Prerif belts along a mesorifan suture [81,82]. These lithologies outcrop 100 km west of the study area. The extension of these rocks to the east as outcrops is unknown, but different types of mantellic and gabbroic xenoliths have been found in lamprophyres, testifying to the existence of these lithologies at depth. This is consistent with the fact that the Guercif Basin constitutes the extension towards the east of the referred-to mesorifan suture, related to the opening of the central Atlantic Ocean (and probably the Maghrebi Tethys) [48,83]. Moreover, the existence at depth of basic and ultrabasic rocks could be related to this oceanic opening, namely by the exhumation along normal faults of CAMP gabbroic plutons, as well as the final exhumation

of the mantle during the Upper Jurassic [47]. As the geochemical signature of these waters implies interaction with basic and ultrabasic rocks placed below the Guercif Basin, they can either have interacted with ophiolites, reflected by the pattern of these waters compared to that of [34] (Figure 8), or with CAMP-affiliated basic and ultrabasic rocks. These hypotheses can only be verified when geophysical data and/or core drilling become available.

5. Conclusions

The Guercif Basin is a geothermal site that offers significant evidence of volcanic-geothermal activity at a surface or near-surface level, whether regarding magmatic (Plio-Quaternary basaltic and trachy-andesitic flows) or hydrothermal (Goutitir thermal spring) activity. The geological, structural, and hydrogeochemical study of the waters of the thermal spring of Goutitir allowed us to better understand the hydrogeological mechanisms at the origin of this source, as well as the processes of water–rock interactions occurring at different levels within the several intersected reservoirs. It was possible to conclude the following:

- The isotopic results reveal that these waters are of meteoric origin and that their recharge zones are estimated at altitudes around 2000 m. These altitudes can only be found SW of the Goutitir thermal spring in the Middle Atlas;
- Water–rock interactions must have taken place along the pathways between the recharge zones in the Middle Atlas and the Guercif Basin through large-scale lithospheric faults such as SMAF and CMAF;
- The groundwater circulation of this hydrothermal system was estimated at a depth of 3.5 km and characterized by water–rock interactions with mafic and mantle igneous rocks present in the basement of the Neogene Guercif Basin;
- The estimated depth is significantly deeper than the Mesozoic reservoir, located at an estimated maximum depth of 2 km, which is often considered the main reservoir in the Atlas domain [14–16,84–86]. These novel results are in agreement with those mentioned for the thermal springs located on the South Rif Thrust [6–8];
- Structural analysis confirms a close relationship between the thermal waters of Goutitir and the intersection between the NE–SW fault network and E–W thrusts, emphasizing on the one hand the relevance of the NE–SW faults as preferential routes for groundwater circulation, and on the other hand the importance of the E–W thrusts to provide ascent structures for the thermo-mineral waters towards the surface (Figure 12).

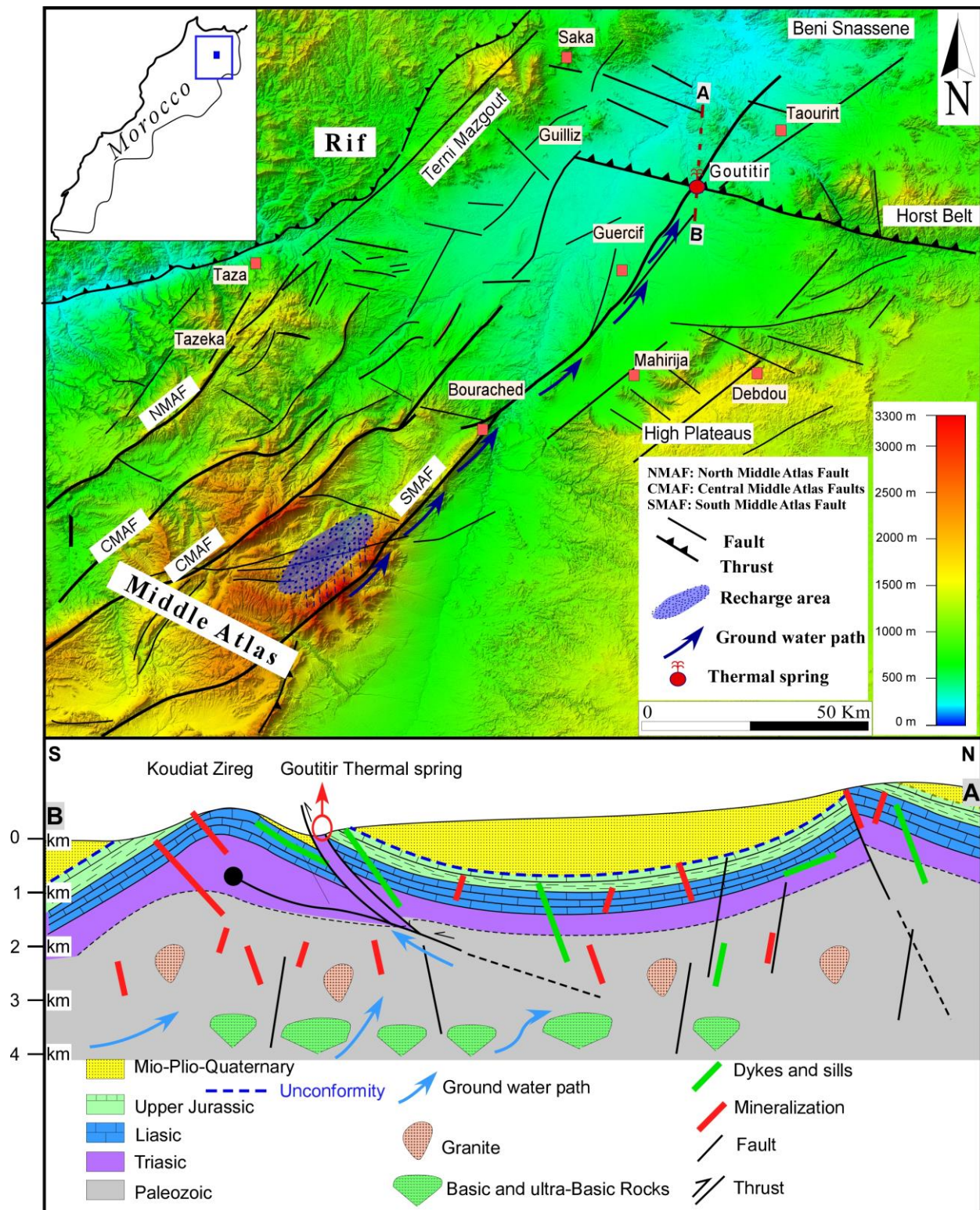


Figure 12. Schematic structural map of the north of Morocco, showing the zones of probable recharge (blue zones) and paths of the groundwater flow (blue arrows) of the studied thermomineral water of the Goutitir, as well as a schematic cross section (A-B) showing the lithological background along with the recharge path of the spring water.

Author Contributions: Conceptualization, A.N.; methodology, E.M.J.; Validation, A.N., T.M.B.d.S. and E.A.F.d.S.; Formal analysis, M.d.R.C.; Investigation, E.M.J., A.N., M.d.R.C., T.M.B.d.S., M.E., Y.D., B.M., N.N., M.H.S. and M.D.; Data curation, E.M.J.; Writing—original draft, E.M.J., A.N., M.d.R.C. and T.M.B.d.S.; Writing—review & editing, B.C.; Supervision, A.N., M.d.R.C. and T.M.B.d.S. All authors have read and agreed to the published version of the manuscript.

Funding: This research received no external funding.

Acknowledgments: This work was funded by the Portuguese Fundação para a Ciência e Tecnologia (FCT) I.P./MCTES through national funds (PIDDAC)-UIDB/50019/2020. The authors would like to thank the reviewers for their pertinent remarks and fruitful collaborations.

Conflicts of Interest: The authors declare no conflict of interest.

References

1. Barbier, E. Geothermal energy technology and current status: An overview. *Renew. Sustain. Energy Rev.* **2002**, *6*, 3–65. [[CrossRef](#)]
2. Li, K.; Bian, H.; Liu, C.; Zhang, D.; Yang, Y. Comparison of geothermal with solar and wind power generation systems. *Renew. Sustain. Energy Rev.* **2015**, *42*, 1464–1474. [[CrossRef](#)]
3. Rimi, A.; Zarhloule, Y.; Barkaoui, A.E.; Correia, A.; Carneiro, J.; Verdoya, M.; Lucazeau, F. Towards a de-carbonized energy system in north-eastern Morocco: Prospective geothermal resource. *Renew. Sustain. Energy Rev.* **2012**, *16*, 2207–2216. [[CrossRef](#)]
4. Soltani, M.; Moradi Kashkooli, F.; Souiri, M.; Rafiei, B.; Jabarifar, M.; Gharali, K.; Nathwani, J.S. Environmental, economic, and social impacts of geothermal energy systems. *Renew. Sustain. Energy Rev.* **2021**, *140*, 110750. [[CrossRef](#)]
5. Tassi, F.; Vaselli, O.; Moratti, G.; Piccardi, L.; Minissale, A.; Poreda, R.; Delgado Huertas, A.; Bendkik, A.; Chenakeb, M.; Tedesco, D. Fluid Geochemistry versus Tectonic Setting: The Case Study of Morocco. *Geol. Soc. Lond. Spec. Publ.* **2006**, *262*, 131–145. [[CrossRef](#)]
6. Lakhdar, A.; Ntarmouchant, A.; Ribeiro, M.; Beqqali, M.; El Ouadeihe, K.; Benaabidate, L.; Dahire, M.; Driouche, Y.; Benslimane, A. New Geological and Geochemical Approach of the Moulay Yacoub Hydrothermal Complex (Northern Border of the South Rifain's Furrow). *Commun. Geol.* **2006**, *93*, 185–204.
7. Lakhdar, A.; Ntarmouchant, A.; Ribeiro, M.L.; Beqqali, M.; el Ouadeihe, K.; Benaabidate, L.; Dahire, M.; Driouche, Y.; Benslimane, A. Détermination de l'origine de la minéralisation des eaux thermales de Moulay Yacoub par des approches géologiques et géochimiques. *Rev. Énerg. Renouvelables CER* **2007**, *7*, 81–84.
8. Sabri, K.; Marrero-Diaz, R.; Ntarmouchant, A.; Bento dos Santos, T.; Ribeiro, M.L.; Solá, A.R.; Smaili, H.; Benslimane, A.; Chibout, M.; Pérez, N.M.; et al. Geology and hydrogeochemistry of the thermo-mineral waters of the South Rif Thrust (Northern Morocco). *Geothermics* **2019**, *78*, 28–49. [[CrossRef](#)]
9. Zarhloule, Y. Le gradient géothermique profond du Maroc: Détermination et cartographie. *Bull. Inst. Sci.* **2004**, *26*, 11–25.
10. Kaasalainen, H.; Stefánsson, A. The chemistry of trace elements in surface geothermal waters and steam, Iceland. *Chem. Geol.* **2012**, *330*, 60–85. [[CrossRef](#)]
11. Wrage, J.; Tardani, D.; Reich, M.; Daniele, L.; Arancibia, G.; Cembrano, J.; Sánchez-Alfaro, P.; Morata, D.; Pérez-Moreno, R. Geochemistry of thermal waters in the Southern Volcanic Zone, Chile—Implications for structural controls on geothermal fluid composition. *Chem. Geol.* **2017**, *466*, 545–561. [[CrossRef](#)]
12. Giggenbach, W.; Sheppard, D.; Robinson, B.; Stewart, M.; Lyon, G. Geochemical structure and position of the Waiotapu geothermal field, New Zealand. *Geothermics* **1994**, *23*, 599–644. [[CrossRef](#)]
13. Wang, M.; Zhou, X.; Liu, Y.; Xu, H.; Wu, Y.; Zhuo, L. Major, trace and rare earth elements geochemistry of geothermal waters from the Rehai high-temperature geothermal field in Tengchong of China. *Appl. Geochem.* **2020**, *119*, 104639. [[CrossRef](#)]
14. Cidu, R.; Bahaj, S. Geochemistry of Thermal Waters from Morocco. *Geothermics* **2000**, *29*, 407–430. [[CrossRef](#)]
15. Benmakhlouf, Mohammed Les Sources Thermales Du Maroc Septentrional: Relation Entre La Tectonique et Le Thermalisme «Northern Moroccan Thermal Springs: The Relationship between Tectonics and Thermalism». Thèse d'Etat, University Mohammed V-Agdal, Fac. Sci., Rabat, Morocco, 2001. Available online: https://www.researchgate.net/profile/Mohamed-Benmakhlouf/publication/273293077_sources_thermales_du_Maroc_relation_entre_le_thermalisme_et_la_tectonique/links/54fd794b0cf20700c5eba84d/sources-thermales-du-Maroc-relation-entre-le-thermalisme-et-la-tectonique.pdf (accessed on 22 September 2001).
16. Jilali, A.; Chamrar, A.; El Haddar, A. Hydrochemistry and geothermometry of thermal water in northeastern Morocco. *Geotherm. Energy* **2018**, *6*, 9. [[CrossRef](#)]
17. Rezouki, I.; Boujamaoui, M.; Hafid, M.; Bba, A.N.; Amiri, A.; Inoubli, M.H.; Manar, A.; Rouai, M.; Baidder, L.; Asebriy, L. Contribution of gravity and aeromagnetic data to the structural modeling of the hidden faults in Guercif Basin, northeastern Morocco. *J. Afr. Earth Sci.* **2020**, *164*, 103797. [[CrossRef](#)]
18. Ajaji, T.; Weis, D.; Giret, A.; Bouabdellah, M. Coeval potassic and sodic calc-alkaline series in the post-collisional Hercynian Tanncherfi intrusive complex, northeastern Morocco: Geochemical, isotopic and geochronological evidence. *Lithos* **1998**, *45*, 371–393. [[CrossRef](#)]

19. Torbi, A. Stratigraphie et évolution structurale paléozoïque d'un segment de la Meseta orientale marocaine (Monts du Sud-Est d'Oujda): Rôle des décrochements dans la formation de l'olistostrome intraviséen et le plutonisme tardi-hercynien. *J. Afr. Earth Sci.* **1996**, *22*, 549–563. [[CrossRef](#)]
20. Bernini, M.; Boccaletti, M.; Gelati, R.; Moratti, G.; Papani, G.; Mokhtari, J.E. Tectonics and Sedimentation In The Taza-Guercif Basin, Northern Morocco: Implications For The Neogene Evolution Of The Rif-Middle Atlas Orogenic System. *J. Pet. Geol.* **1999**, *22*, 115–128. [[CrossRef](#)]
21. Michard, A.; Hoepffner, C.; Soulaïmani, A.; Baidder, L. The Variscan Belt. In *Continental Evolution: The Geology of Morocco*; Lecture Notes in Earth Sciences; Michard, A., Saddiqi, O., Chalouan, A., de Lamotte, D.F., Eds.; Springer Berlin Heidelberg: Berlin, Heidelberg, 2008; Volume 116, pp. 65–132, ISBN 978-3-540-77075-6.
22. GIRET, P. Histoire Paléogéographique, Pétrologique et Structurale Du District à Fluorine de Taourirt (Maroc Oriental). «Paleo-geographic, Petrological and Structural History of the Taourirt Fluorite District». Ph.D. Thesis, University of Orléans, Orléans, France, 1985; 191 p.
23. Laville, E.; Delcaillau, B.; Charroud, M.; Dugué, O.; Ait Brahim, L.; Cattaneo, G.; Deluca, P.; Bouazza, A. The Plio-Pleistocene Evolution of the Southern Middle Atlas Fault Zone (SMAFZ) Front of Morocco. *Int. J. Earth Sci. (Geol. Rundsch.)* **2007**, *96*, 497–515. [[CrossRef](#)]
24. Rakus, M. Evolution et Position Paléogéographique Des Monts d'Oujda Au Cours Du Mésozoïque. «Evolution and Paleogeographic Position of the Oujda Mounts During the Mesozoic». *Unpubl. Rep. Mines Géol Et Energ. Rabat* **1979**, *46*, 75–78.
25. Charroud, M. Evolution Géodynamique Des Hauts Plateaux (Maroc) et de Leurs Bordures Du Mésozoïque Au Cénozoïque «Geodynamic Evolution of the High Plateaux (Morocco) and Their Boundaries from Mesozoic to Cenozoic». Ph.D Thesis, Univeraity Sidi Mohamed Ben Abdellah, Fès, Morocco, 2002; p. 314.
26. Laville, E.; Fedan, B. Le Système Atlasique Marocain Au Jurassique: Évolution Structurale et Cadre Géodynamique « The Moroccan Atlas System in the Jurassic Period: Structural Evolution and Geodynamic Framework». *Sci. Géologiques Bull. Mémoires* **1989**, *84*, 3–28.
27. Fedan, B.; Laville, E.; El Mezgueldi, A. Le Bassin Jurassique Du Moyen Atlas (Maroc); Exemple de Bassin Sur Relais de Decrochements «The Middle Atlas Jurassic Basin (Morocco); Example of a Basin on strike-slip Relay». *Bull. De La Soc. Géologique De Fr.* **1989**, *12*, 1123–1136. [[CrossRef](#)]
28. Nassili, M. Evolution Géodynamique Comparée Des Séries Jurassiques (Lias-Dogger) Du Pourtour Du Bassin de Guercif (Moyen Atlas, Hauts Plateaux et Zone de Taourirt–Maroc Nord Oriental). «Comparative Geodynamic Evolution Of The Jurassic (Lias-Dogger) Series Around The Guercif Basin (Middle Atlas, High Plateaux and Taourirt-Northern Morocco Zone)». Ph.D. Thesis, Université Mohammed V, Rabat, Morocco, 2006; p. 309.
29. Hssaida, T.; Benzaggagh, M.; Riding, J.B.; Huault, V.; Essamoud, R.; Mouflih, M.; Jaydawi, S.; Chakir, S.; Nahim, e.M. Répartition stratigraphique et biozones des kystes de dinoflagellés au passage Jurassique moyen–Jurassique supérieur (Bathonien supérieur–Oxfordien inférieur) dans le Bassin de Guercif, Maroc nord-oriental. *Ann. Paléontol.* **2017**, *103*, 197–215. [[CrossRef](#)]
30. Bernini, M.; Boccaletti, M.; Moratti, G.; Papani, G. Structural development of the Taza-Guercif Basin as a constraint for the Middle Atlas Shear Zone tectonic evolution. *Mar. Pet. Geol.* **2000**, *17*, 391–408. [[CrossRef](#)]
31. Krijgsman, W.; Langereis, C.G.; Zachariasse, W.J.; Boccaletti, M.; Moratti, G.; Gelati, R.; Iaccarino, S.; Papani, G.; Villa, G. Late Neogene evolution of the Taza–Guercif Basin (Rifian Corridor, Morocco) and implications for the Messinian salinity crisis. *Mar. Geol.* **1999**, *153*, 147–160. [[CrossRef](#)]
32. Colletta, B. *Evolution Néotectonique de la Partie Méridionale du Bassin de Guercif (Maroc Oriental)*; Université Scientifique et Médicale de Grenoble: Grenoble, France, 1979; pp. 439–464.
33. Sasvári, Á.; Baharev, A. SG2PS (structural geology to postscript converter)—A graphical solution for brittle structural data evaluation and paleostress calculation. *Comput. Geosci.* **2014**, *66*, 81–93. [[CrossRef](#)]
34. D'Amore, F.; Scandiffio, G.; Panichi, C. Some observations on the chemical classificatin of ground waters. *Geothermics* **1983**, *12*, 141–148. [[CrossRef](#)]
35. Verma, S.P.; Pandarinath, K.; Santoyo, E. SolGeo: A new computer program for solute geothermometers and its application to Mexican geothermal fields. *Geothermics* **2008**, *37*, 597–621. [[CrossRef](#)]
36. Reed, M.; Spycher, N. Calculation of pH and mineral equilibria in hydrothermal waters with application to geothermometry and studies of boiling and dilution. *Geochim. Cosmochim. Acta* **1984**, *48*, 1479–1492. [[CrossRef](#)]
37. Parkhurst, D.L.; Appelo, C.A.J. *User's Guide to PHREEQC (Version 2): A Computer Program for Speciation, Batch-Reaction, One-Dimensional Transport, and Inverse Geochemical Calculations*; Water-Resources Investigations Report; U.S. Geological Survey: Washington, DC, USA, 1999.
38. Giggensbach, W.F. Geothermal solute equilibria. Derivation of Na-K-Mg-Ca geoindicators. *Geochim. Cosmochim. Acta* **1988**, *52*, 2749–2765. [[CrossRef](#)]
39. Giret, P.; Touray, J.-C.; Ildefonse, J.-P.; Jebrak, M. Dynamique de mise en place des extrusions monoclinales liasiques de la region de Taourirt (Maroc oriental); l'apport d'une etude d'inclusions fluides. *Bull. Société Géologique Fr.* **1985**, *1*, 787–790. [[CrossRef](#)]
40. Bouziane, A.B. Stratigraphie et Sedimentologie du Lias et du Dogger Inferieur du Bassin de Guercif «Liassic and Early Dogger Stratigraphy and Sedimentology of the Guercif Basin». Ph.D Thesis, Université Claude Bernard Lyon-1, Lyon, France, 1984.
41. Torbi, A. Déformations Cassantes et Paléo-Champs de Contrainte Enregistrés dans les Terrains Mésocénozoïques du Maroc Nord-oriental: Etude par la Microfracturation, Conséquences Géodynamiques et Cinématiques. «Brittle Deformations and Paleo

- Stress Fields Recorded in the Mesocenoic Terrains of Northeastern Morocco: Microfracturing Study, Geodynamic and Kinematic Consequences». Ph.D. Thesis, Université Mohammed Premier, Oujda, Morocco, 1997; p. 279.
42. Wagner, C.; Mokhtari, A.; Deloule, E.; Chabaux, F. Carbonatite and Alkaline Magmatism in Taourirt (Morocco): Petrological, Geochemical and Sr–Nd Isotope Characteristics. *J. Petrol.* **2003**, *44*, 937–965. [[CrossRef](#)]
 43. Mokhtari, A.; Velde, D. Xenocrysts in Eocene camptonites from Taourirt, northern Morocco. *Mineral. Mag.* **1988**, *52*, 587–601. [[CrossRef](#)]
 44. Hernandez, J.; Bellon, H. Chronologie K–Ar du volcanisme miocène du Rif oriental (Maroc): Implications tectoniques et magmatologiques. *Rev. Géologie Dyn. Géographie Phys.* **1985**, *26*, 85–94.
 45. Gomez, F.; Barazangi, M.; Demnati, A. Structure and Evolution of the Neogene Guercif Basin at the Junction of the Middle Atlas Mountains and the Rif Thrust Belt, Morocco. *AAPG Bull.* **2000**, *84*, 865. [[CrossRef](#)]
 46. Sani, F.; Zizi, M.; Bally, A.W. The Neogene–Quaternary evolution of the Guercif Basin (Morocco) reconstructed from seismic line interpretation. *Mar. Pet. Geol.* **2000**, *17*, 343–357. [[CrossRef](#)]
 47. Escosa, F.O.; Leprêtre, R.; Spina, V.; Gimeno-Vives, O.; Kergaravat, C.; Mohn, G.; Frizon de Lamotte, D. Polyphased mesozoic rifting from the Atlas to the north-west Africa paleomargin. *Earth-Sci. Rev.* **2021**, *220*, 103732. [[CrossRef](#)]
 48. Gimeno-Vives, O.; de Lamotte, D.F.; Leprêtre, R.; Haissen, F.; Atouabat, A.; Mohn, G. The structure of the Central-Eastern External Rif (Morocco); Poly-phased deformation and role of the under-thrusting of the North-West African paleo-margin. *Earth-Sci. Rev.* **2020**, *205*, 103198. [[CrossRef](#)]
 49. Chalouan, A. *Continental Evolution: The Geology of Morocco: Structure, Stratigraphy, and Tectonics of the Africa-Atlantic-Mediterranean Triple Junction*; Michard, A., Saddiqi, O., Chalouan, A., de Lamotte, D.F., Eds.; Lecture Notes in Earth Sciences; Springer Berlin/Heidelberg: Berlin, Germany, 2008; Volume 116, ISBN 978-3-540-77075-6.
 50. Tejera de Leon, J.; Duée, G. Relationships between the Neogene foredeep basins of the Western external Rifian belt related to the Arbaoua-Jebha transform fault. Consequences for the interpretation of the evolution of the Rifian belt (Morocco). *Inst. Sci. Rabat. Sér. Géol. Géogr. Phys.* **2003**, *21*, 1–19.
 51. Chalouan, A.; Michard, A.; Kadiri, K.E.; Negro, F.; de Lamotte, D.F.; Soto, J.I.; Saddiqi, O. The Rif Belt. In *Continental Evolution: The Geology of Morocco*; Michard, A., Saddiqi, O., Chalouan, A., de Lamotte, D.F., Eds.; Lecture Notes in Earth Sciences; Springer Berlin Heidelberg: Berlin/Heidelberg, Germany, 2008; Volume 116, pp. 203–302, ISBN 978-3-540-77075-6.
 52. Torbi, A.; Gélard, J.-P. Palaeostresses identified in the Meso-Cenozoic cover of northeastern Morocco. Relationship with the opening of the Atlantic ocean and the kinematics of the African and European plates. *Comptes Rendus Académie Sci.-Ser. IIA-Earth Planet. Sci.* **2000**, *330*, 853–858. [[CrossRef](#)]
 53. Frizon de Lamotte, D.; Saint Bezar, B.; Bracène, R.; Mercier, E. The two main steps of the Atlas building and geodynamics of the western Mediterranean. *Tectonics* **2000**, *19*, 740–761. [[CrossRef](#)]
 54. Gomez, F.; Beauchamp, W.; Barazangi, M. Role of the Atlas Mountains (northwest Africa) within the African-Eurasian plate-boundary zone. *Geology* **2000**, *28*, 775–778. [[CrossRef](#)]
 55. Boufkri, H.; El Azzab, D.; Miftah, A.; Mohammed, C. Identifications and geodynamic implications of magnetic structures of the Oujda-Debdou-Guercif zone (North-Eastern of Morocco): Analysis and processing of aeromagnetic data. *Arab. J. Geosci.* **2021**, *14*, 2241. [[CrossRef](#)]
 56. Zizi, M. *Triassic-Jurassic Extensional Systems and Their Neogene Reactivation in Northern Morocco (the Rides Prérifaines and Guercif Basin)*; Rice University: Houston, TX, USA, 1996; ISBN 9798208914328.
 57. Durov, S. Natural waters and graphic representation of their composition. *Dokl. Akad. Nauk. SSSR* **1948**, *59*, 87–90.
 58. Et-Touhami, M. Lithostratigraphy and depositional environments of Lower Mesozoic evaporites and associated red beds, Khemisset Basin, northwestern Morocco. *Zent. Geol. Palaontol. Teil. I* **2000**, *1998*, 1193–1216.
 59. Bouabdellah, M.; Castorina, F.; Bodnar, R.J.; Banks, D.; Jebrak, M.; Prochaska, W.; Lowry, D.; Klugel, A.; Hoernle, K. Petroleum Migration, Fluid Mixing, and Halokinesis as the Main Ore-Forming Processes at the Peridiapiric Jbel Tirremi Fluorite-Barite Hydrothermal Deposit, Northeastern Morocco. *Econ. Geol.* **2014**, *109*, 1223–1256. [[CrossRef](#)]
 60. Pasvanoğlu, S.; Chandrasekharam, D. Hydrogeochemical and isotopic study of thermal and mineralized waters from the Nevşehir (Kozakli) area, Central Turkey. *J. Volcanol. Geotherm. Res.* **2011**, *202*, 241–250. [[CrossRef](#)]
 61. Aydin, H.; Karakuş, H.; Mutlu, H. Hydrogeochemistry of geothermal waters in eastern Turkey: Geochemical and isotopic constraints on water-rock interaction. *J. Volcanol. Geotherm. Res.* **2020**, *390*, 106708. [[CrossRef](#)]
 62. McDonough, W.F.; Sun, S.-S. The composition of the Earth. *Chem. Evol. Mantle* **1995**, *120*, 223–253. [[CrossRef](#)]
 63. Pantić, T.P.; Birke, M.; Petrović, B.; Nikolov, J.; Dragišić, V.; Živanović, V. Hydrogeochemistry of thermal groundwaters in the Serbian crystalline core region. *J. Geochem. Explor.* **2015**, *159*, 101–114. [[CrossRef](#)]
 64. Apollaro, C.; Marini, L.; Critelli, T.; Barca, D.; Bloise, A.; De Rosa, R.; Liberi, F.; Miriello, D. Investigation of rock-to-water release and fate of major, minor, and trace elements in the metabasalt–serpentinite shallow aquifer of Mt. Reventino (CZ, Italy) by reaction path modelling. *Appl. Geochem.* **2011**, *26*, 1722–1740. [[CrossRef](#)]
 65. Georgopoulos, G.; Mitsis, I.; Argyraki, A.; Stamatakis, M. Environmental availability of ultramafic rock derived trace elements in the fumarolic–Geothermal field of Soussaki area, Greece. *Appl. Geochem.* **2018**, *92*, 9–18. [[CrossRef](#)]
 66. Perraki, M.; Vasileiou, E.; Bartzas, G. Tracing the origin of chromium in groundwater: Current and new perspectives. *Curr. Opin. Environ. Sci. Health* **2021**, *22*, 100267. [[CrossRef](#)]

67. Bouri, S.; Gasmi, M.; Jaouadi, M.; Souissi, I.; Mimi, A.L.; Dhia, H.B. Etude intégrée des données de surface et de subsurface pour la prospection des bassins hydrogéothermiques: Cas du bassin de Maknassy (Tunisie centrale)/Integrated study of surface and subsurface data for prospecting hydrogeothermal basins: Case of the Maknassy basin (central Tunisia). *Hydrol. Sci. J.* **2007**, *52*, 1298–1315. [[CrossRef](#)]
68. Fournier, R.O. A Revised Equation for the Na/K Geothermometer. *Trans. Geotherm. Resour. Counc.* **1979**, *3*, 221–224.
69. Arnórsson, S. Isotopic and chemical techniques in geothermal exploration, development and use. *Int. At. Energy Agency* **2000**, *15*, 109–111.
70. Verma, S.P.; Santoyo, E. New improved equations for NaK, NaLi and SiO₂ geothermometers by outlier detection and rejection. *J. Volcanol. Geotherm. Res.* **1997**, *79*, 9–23. [[CrossRef](#)]
71. Fournier, R.O.; Truesdell, A.H. An empirical Na K Ca geothermometer for natural waters. *Geochim. Cosmochim. Acta* **1973**, *37*, 1255–1275. [[CrossRef](#)]
72. Nieva, D.; Nieva, R. Developments in geothermal energy in Mexico—Part twelve. A cationic geothermometer for prospecting of geothermal resources. *Heat Recovery Syst. CHP* **1987**, *7*, 243–258. [[CrossRef](#)]
73. Kharaka, Y.K.; Mariner, R.H. Chemical Geothermometers and Their Application to Formation Waters from Sedimentary Basins. In *Thermal History of Sedimentary Basins*; Naeser, N.D., McCulloh, T.H., Eds.; Springer New York: New York, NY, USA, 1989; pp. 99–117, ISBN 978-1-4612-8124-5.
74. Craig, H. Isotopic variations in meteoric waters. *Science* **1961**, *133*, 1702–1703. [[CrossRef](#)]
75. Raïbi, F.; Benkaddour, A.; Hanich, L.; Chehbouni, A.; Chtioui, M. Variation de la composition des isotopes stables des précipitations en climat semi-aride (cas du bassin-versant de Tensift Maroc). *GIRE3D Marrakech Maroc* **2006**, *75*, 9.
76. Bouchaou, L.; Tagma, T.; Boutaleb, S.; Hsissou, Y.; Nathaniel, W.; Vengosh, A.; Michelot, J.; Massault, M.; Elfaskaoui, M. Isotopic Composition and Age of Surface Water as Indicators of Groundwater Sustainability in a Semiarid Area: Case of the Souss Basin (Morocco). In *Proceedings of the International Symposium on Isotopes in Hydrology, Marine Ecosystems and Climate Change Studies*, Monaco, 27 March–1 April 2011.
77. Bouchaou, L.; Warner, N.R.; Tagma, T.; Hssaisoune, M.; Vengosh, A. The origin of geothermal waters in Morocco: Multiple isotope tracers for delineating sources of water-rock interactions. *Appl. Geochem.* **2017**, *84*, 244–253. [[CrossRef](#)]
78. Winckel, A.; Marlin, C.; Dever, L.; Morel, J.-L.; Morabiti, K.; Makhlof, M.B.; Chalouan, A. Apport des isotopes stables dans l'estimation des altitudes de recharge de sources thermales du Maroc. «Recharge altitude estimation of thermal springs using stable isotopes in Morocco». *Comptes Rendus Geosci.* **2002**, *334*, 469–474. [[CrossRef](#)]
79. Ármannsson, H.; Benjamínsson, J.; Jeffrey, A.W.A. Gas changes in the Krafla geothermal system, Iceland. *Water-Rock Interact.* **1989**, *76*, 175–196. [[CrossRef](#)]
80. Allard, P. The origin of hydrogen, carbon, sulfur, nitrogen and rare gases in volcanic exhalations: Evidence from isotope geochemistry. *Forecast. Volcan. Events* **1983**, *16*, 337–386.
81. Michard, A.; Mokhtari, A.; Chalouan, A.; Saddiqi, O.; Rossi, P.; Rjimati, E.-C. New ophiolite slivers in the External Rif belt, and tentative restoration of a dual Tethyan suture in the western Maghrebides. *Bull. Société Géologique Fr.* **2014**, *185*, 313–328. [[CrossRef](#)]
82. Michard, A.; Saddiqi, O.; Chalouan, A.; Chabou, M.C.; Lach, P.; Rossi, P.; Bertrand, H.; Youbi, N. Comment on “The Mesozoic Margin of the Maghrebian Tethys in the Rif Belt (Morocco): Evidence for Polyphase Rifting and Related Magmatic Activity” by Gimeno-Vives et al. *Tectonics* **2020**, *39*, 4. [[CrossRef](#)]
83. Gimeno-Vives, O.; Mohn, G.; Bosse, V.; Haissen, F.; Zaghoul, M.N.; Atouabat, A.; Frizon de Lamotte, D. Reply to comment by Michard et al. on “The Mesozoic Margin of the Maghrebian Tethys in the Rif Belt (Morocco): Evidence for Polyphase Rifting and Related Magmatic Activity”. *Tectonics* **2020**, *39*, 6165. [[CrossRef](#)]
84. Barkaoui, A.E.; Zarhloule, Y.; Verdoya, M.; Pasquale, V.; Lahrach, H. Progress in understanding the geothermal sedimentary basins in northeastern Morocco. *J. Afr. Earth Sci.* **2014**, *97*, 1–8. [[CrossRef](#)]
85. Barkaoui, A.E.; Zarhloule, Y.; Rimi, A.; Verdoya, M.; Bouri, S. Hydrogeochemical investigations of thermal waters in the northeastern part of Morocco. *Environ. Earth Sci.* **2014**, *71*, 1767–1780. [[CrossRef](#)]
86. Zarhloule, Y.; Bouri, S.; Lahrach, A.; Boughriba, M.; El Mandour, A.; Ben Dhia, H. Hydrostratigraphical study, geochemistry of thermal springs, shallow and deep geothermal exploration in Morocco: Hydrogeothermal potentialities. In *Proceedings of the World Geothermal Congress 2005*, Antalya, Turkey, 24–29 April 2005; pp. 24–29.

Disclaimer/Publisher’s Note: The statements, opinions and data contained in all publications are solely those of the individual author(s) and contributor(s) and not of MDPI and/or the editor(s). MDPI and/or the editor(s) disclaim responsibility for any injury to people or property resulting from any ideas, methods, instructions or products referred to in the content.